

# Anisotropic scaffolds for peripheral nerve and spinal cord regeneration

Wen Xue<sup>a,b</sup>, Wen Shi<sup>a,b</sup>, Yunfan Kong<sup>a,b</sup>, Mitchell Kuss<sup>a,b</sup>, Bin Duan<sup>a,b,c,d,\*</sup>

<sup>a</sup> Mary & Dick Holland Regenerative Medicine Program, University of Nebraska Medical Center, Omaha, NE, USA

<sup>b</sup> Division of Cardiology, Department of Internal Medicine, University of Nebraska Medical Center, Omaha, NE, USA

<sup>c</sup> Department of Surgery, University of Nebraska Medical Center, Omaha, NE, USA

<sup>d</sup> Department of Mechanical Engineering, University of Nebraska-Lincoln, Lincoln, NE, USA

## ARTICLE INFO

### Keywords:

Tissue engineering  
Topography  
Alignment  
Surface pattern  
Hydrogel

## ABSTRACT

The treatment of long-gap (>10 mm) peripheral nerve injury (PNI) and spinal cord injury (SCI) remains a continuous challenge due to limited native tissue regeneration capabilities. The current clinical strategy of using autografts for PNI suffers from a source shortage, while the pharmacological treatment for SCI presents dissatisfactory results. Tissue engineering, as an alternative, is a promising approach for regenerating peripheral nerves and spinal cords. Through providing a beneficial environment, a scaffold is the primary element in tissue engineering. In particular, scaffolds with anisotropic structures resembling the native extracellular matrix (ECM) can effectively guide neural outgrowth and reconnection. In this review, the anatomy of peripheral nerves and spinal cords, as well as current clinical treatments for PNI and SCI, is first summarized. An overview of the critical components in peripheral nerve and spinal cord tissue engineering and the current status of regeneration approaches are also discussed. Recent advances in the fabrication of anisotropic surface patterns, aligned fibrous substrates, and 3D hydrogel scaffolds, as well as their *in vitro* and *in vivo* effects are highlighted. Finally, we summarize potential mechanisms underlying the anisotropic architectures in orienting axonal and glial cell growth, along with their challenges and prospects.

## 1. Introduction

The human nervous system assumes critical roles in transmitting information and signals to and from various parts of body [1]. It is normally divided into the peripheral nervous system (PNS) and the central nervous system (CNS) [1]. With a network of nerves throughout the body, the PNS transfers information between the CNS and the body, while information is analyzed and coordinated by the CNS [2]. Injury to the nervous system is a major cause of pain, sensory disfunctions, and physical and mental impairments [3,4]. More than 2,000,000 people have different forms of peripheral nerve injury (PNI), and approximately 265,000 people live with spinal cord injury (SCI), with 12,000 new cases occurring every year in the United States alone due to accidents, sports, or falls [5,6]. The immense emotional, social, and economic costs desperately call for effective therapeutic strategies.

Although the PNS has an innate regeneration potential after injury, defects longer than 10 mm cannot heal spontaneously [7]. Surgical interventions to prevent a harsh microenvironment and bridge the gap are required. The current clinical standard for long-gap PNI repair is using

autografts [7]. However, this is often limited by size mismatch, source shortage, and permanent damage to the donor site [8]. Distinct from the PNS, the spinal cord has poor regenerative capacity, and, currently, there are still no effective clinical treatments for SCI [9]. Pharmaceutical treatment and palliative functional recovery through rehabilitation are considered as the main options nowadays [10], which unfortunately cannot reverse the damage and restore motor abilities.

Tissue and regeneration engineering aims to replace, repair, or regenerate damaged, degenerated, or defective tissues using engineering approaches, including scaffolds, cells, and biophysical and biochemical stimuli [11]. It demonstrates potential advantages for regenerating peripheral nerves and spinal cords [12]. By applying tissue engineered constructs, the gap of the damaged nerve can be bridged, and axon re-growth is directed [13]. Cells can be incorporated to accelerate vascularization, re-myelination, and synaptic reorganization, as well as to provide paracrine-signaling factors [14]. Stimuli, like mechanical, chemical, and electrical cues, have also been applied to mimic the physiological microenvironment and promote regeneration after PNI and SCI [15].

Peer review under responsibility of KeAi Communications Co., Ltd.

\* Corresponding author. Mary & Dick Holland Regenerative Medicine Program, University of Nebraska Medical Center, Omaha, NE, USA

E-mail address: [bin.duan@unmc.edu](mailto:bin.duan@unmc.edu) (B. Duan).

<https://doi.org/10.1016/j.bioactmat.2021.04.019>

Received 2 March 2021; Received in revised form 5 April 2021; Accepted 13 April 2021

2452-199X/© 2021 The Authors. Publishing services by Elsevier B.V. on behalf of KeAi Communications Co. Ltd. This is an open access article under the CC

BY-NC-ND license (<http://creativecommons.org/licenses/by-nc-nd/4.0/>).

Among various components, a scaffold provides a three-dimensional (3D) platform and a beneficial environment for peripheral nerve and spinal cord regeneration and is the primary element in tissue engineering [16]. An ideal nerve scaffold should satisfy many biological and physicochemical requirements, such as biocompatibility, degradability, sufficient biomechanics, and suitable porosity [13]. In addition, it is essential for the nerve tissue engineering scaffolds to provide an anisotropic structure resembling the native extracellular matrix (ECM), conferring cell orientation, and guiding axon growth and reconnection [17]. Failure to recreate the anisotropic architecture of nerves is a limitation in clinical repair and regeneration [17]. A variety of approaches have thus been developed to achieve anisotropic structures on surfaces, fibrous substrates, and hydrogel scaffolds.

In this review, we focus on the fabrication and function of anisotropic topography and scaffolds, which show longitudinal direction dependent physical or structural features (where alignment is an example of anisotropic features), in regenerating long-gap PNI (>10 mm) and SCI. We first offer an overview of the anatomies of native peripheral nerves and spinal cords as well as critical requirements for regenerative scaffold designs. We then focus on reviewing various fabrication methods and recent advances of anisotropic nerve scaffolds from multidimensional aspects, i.e. anisotropic surface patterns (considered as one dimension-1D), anisotropic aligned fibrous substrates (two dimensions-2D), and 3D anisotropic hydrogel scaffolds. The effects of anisotropic architectures on *in vitro* and *in vivo* functions are also discussed. Furthermore, we delineate potential mechanisms of anisotropic architectures in orienting axon and glial cell growth. Finally, challenges and prospects of applying anisotropic topographies and scaffolds to nerve regeneration are highlighted.

## 2. Peripheral nerve and spinal cord regeneration strategies

### 2.1. Anatomy of the spinal cord and peripheral nerve

The human nervous system can be divided into two interacting subsystems: the PNS and the CNS. The CNS consists of the brain and spinal cord [18]. The spinal cord is located in the center of the spine, surrounded by bones (vertebrae), discs, muscles, and ligaments [19]. It links the brain and different parts of the body [20]. The human spinal cord is a cylindrical structure that is 40–50 cm in length and 1–1.5 cm in diameter and is made up of gray and white matters [18] (Fig. 1). The

front 2 Gy matters contain neurons transmitting information from the brain to the PNS, while the back two transmit information from the PNS to the brain. The surrounding white matter contains tracts, which are bundles of parallel axons with similar functions, that convey information to or from the brain [21]. Apart from neurons, glial cells, including astrocytes, oligodendrocytes, and microglia, are also present in the spinal cord. Astrocytes have a star like morphology and help maintain chemical environment stability in the spinal cord via various methods, like removing excessive potassium ions and recycling neurotransmitters [19]. They have numerous projections that connect neurons with surrounding blood vessels. Oligodendrocytes produce a fatty myelin wrapping around axons, allowing more efficient electrical signal transduction. Microglial cells are smaller in size and work like macrophages in the PNS by removing cell debris [19]. Also, blood vessels surround the spinal cord along the entire length [22]. Starting from the spinal cord, there are 31 pairs of spinal nerves [23]. They are part of the PNS, and each pair of spinal nerves is the combination of axons from the dorsal and ventral roots. The dorsal root is the afferent sensory root and carries information to the brain, while the ventral root is the efferent root and carries information from the brain [24]. Neurons with cell bodies in the dorsal root comprise the dorsal root ganglion (DRG) [25,26], which carry sensory neural signals to the CNS.

Beginning with spinal nerves, the PNS connects the spinal cord to the rest of body to maintain sensation and movement. For peripheral neurons, groups of parallel axons myelinated by Schwann cells (SCs) form fascicles, and these fascicles are protected by collagenous fiber endoneurium [27] (Fig. 1). Further, perineurium, composed of layers of collagen membrane and sheets of perineurial cells, surrounds the fascicles [27]. Several fascicles and blood vessels are further enclosed into the epineurium, consisting of collagen fibers and lipid globules. Blood vessels surrounding the axons provide nutrition and mass exchange [27].

After an SCI, numerous cascades are triggered in the body in a timely manner [28–30] (Fig. 2A). First, neurons and glial cells die, and blood vessels rupture after primary injury, where the injury happens. Then, it is followed by secondary injury, during which inflammatory cells (including neutrophils, microglia, macrophages, and T cells) clean cell debris, and a glial scar forms to protect the injured spinal cord from further infection and cell damage. The glial scar facilitates blood supply re-establishment [31]. Once the injury slows, spontaneous healing happens, consisting of limited axon sprouting and blood vessel

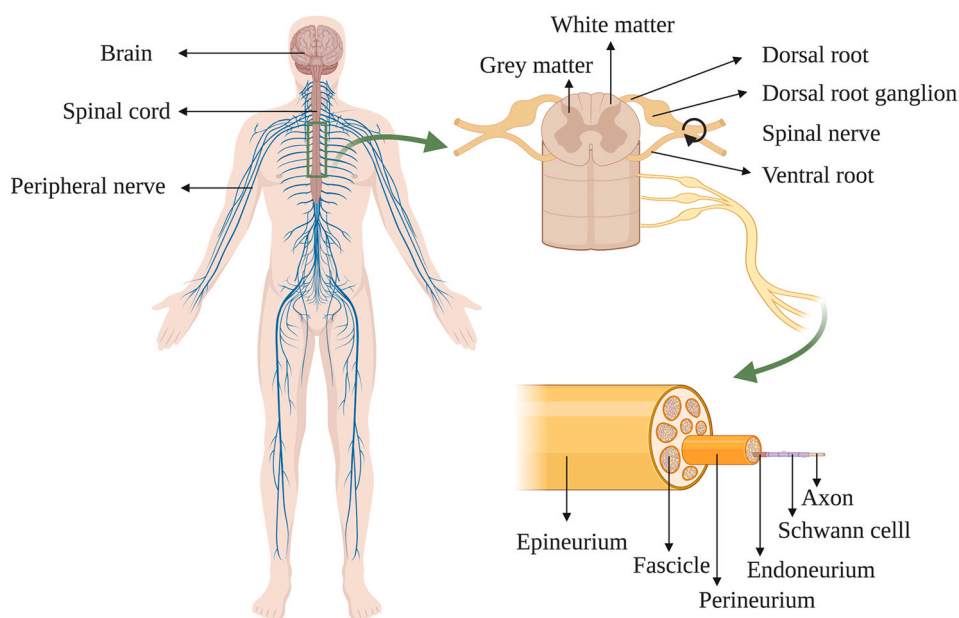


Fig. 1. Schematic of the human spinal cord and peripheral nerve anatomy.

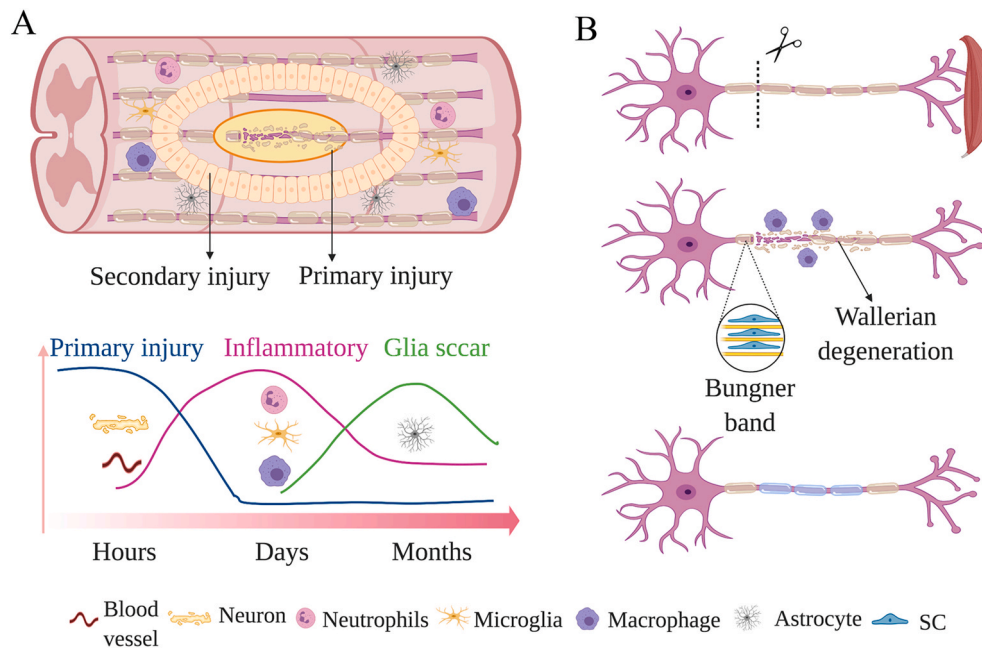


Fig. 2. Physiological changes after SCI (A) and PNI (B) at the injury site.

formation [32]. Despite the glial scar's advantage in injury prevention, it impedes neuron regrowth. The ECM produced by scar related cells contain axon growth inhibitors, like chondroitin-sulfates and proteoglycans [31]. This is one of the reasons neuron regeneration is limited after SCI.

A PNI also results in a cascade of physiological changes at the injury site (Fig. 2B). The distal end of the axon undergoes swelling, myelin breakdown, and axon degeneration, which is called Wallerian degeneration [33]. Under severe or long-gap defects, inflammatory cells cause fibrous dense scarring [34]. At the proximal end, regeneration initiates by forming Büngner bands after degenerative changes (SCs demyelination and macrophage activation) [35]. Büngner bands, composed of longitudinally oriented SCs, guide axon regrowth towards the distal end [36]. For injuries without nerve continuity damage, neurite regrowth can be achieved spontaneously through Büngner bands. However, for serious injuries, dense scars, consisting of SCs, fibroblasts, macrophages, and collagenous ECMs and caused by significant inflammation and disorganized proximal ends result in the failure of regeneration [37].

## 2.2. Clinical strategies for the treatment and management of PNI and SCI

In response to small injuries without damage to nerve continuity in PNI, peripheral nerves can regenerate instinctively following a series of pathophysiological reactions [13,38]. For injuries with nerve transection, direct suturing without grafting is the gold-standard treatment for peripheral nerves with short gap (<5 mm) injuries [13]. Sutureless repair by using fibrin glue is another option to ensure a shorter recovery time [13]. There is no significant difference between suturing and gluing approaches when evaluating axonal regeneration, fiber alignment, and nerve conduction recovery [13].

Larger defects require nerve grafting, and using autologous sensory nerves is the gold-standard. Autografts demonstrate considerable recovery results, especially in long-gap injuries (>3 cm) [39,40]. However, several limitations are associated with the implementation of autografts, including scarcity of the tissue source, second surgery trauma, donor-site function loss and morbidity, and mismatches in tissue size [8]. An allograft from a cadaver or donor is an alternative option. Although the recovery results are reasonable, sustained immunosuppressive therapy costs a lot and can potentially induce infection and tumor [13]. Acellular grafts, which are made by using

physical, chemical, and enzymatic methods to remove cells but preserve the nerve structure and ECM, decrease the immune response while helping regeneration. Avance® is one of decellularized nerve grafts approved by the food and drug administration (FDA) [41]. Recently, more research has focused on the development of synthetic nerve scaffolds as alternatives. For this purpose, ideal nerve scaffolds should have properties like biocompatibility, biodegradability, permeability, flexibility, proper mechanics, and appropriate surface performance. Currently, there are many synthetic scaffolds made from collagen (NeuraGen®, NeuroFlex®, NeuroMatrix®, NeuraWrap®, NeuroMend®), polyglycolic acid (PGA) (NeuroTube®), polyvinyl alcohol (PVA) (SaluTunnel®), and other materials that have been approved by FDA [42], but their application is still restricted to nerve defects shorter than 3 cm.

Spinal cords show limited self-healing abilities after injury. At the primary injury and inflammation stage, pharmacological treatment, like neuroprotective and anti-inflammatory drugs (riluzole, ketorolac, minocycline, etc.), is suggested [43]. Decompression surgery, to remove discs or bone fragments, and blood pressure augmentation are also adopted to protect cells from further damage [43]. Substantial efforts in clinical trials have been devoted to cell transplantations using stem cells, like neural stem cells (NSC), hematopoietic stem cells (HSC), mesenchymal stem cells (MSC), and glial cells like SCs, to help spinal cord regeneration during or after the secondary injury stage [44,45]. However, the therapeutic effects of cell transplantation are limited by a low cell survival rate [46]. Scaffolds offering protective environments and proper mechanical performances are promising to bridge injured spinal cords and increase the encapsulated cell survival rate. FDA approved polymers, like collagen, have been applied as scaffold components for SCI treatment trials [44].

## 2.3. Regeneration of peripheral nerves and spinal cords through tissue engineered approaches

There are two main scaffold-involving tissue engineering approaches for regenerating peripheral nerves and spinal cords. One is with the encapsulation of cells, which involves seeding or encapsulating cells on or within the scaffolds *in vitro* and then implanting them into the injury site [14,47]. The other one is the application of cell-free biomaterials with growth factors or other biomolecules that will be released to recruit

cells *in situ* [48].

Supporting cells in cell-based therapy include autologous mature cells and stem cells, as listed in Table 1. SCs are the key glial cells in the PNS. They wrap around the axons, form a myelin sheath, and produce neurotrophic factors like nerve growth factor (NGF) [49], which may promote nerve regeneration. Studies also demonstrate that SC implantation is helpful for damaged spinal cord repair [50,51]. Glial cells in the CNS, like astrocytes and oligodendrocytes, have been adopted in some pre-clinical studies for spinal cord recovery, and they show significant improvement in functional recovery after SCI [52,53]. Stem cells, like NSCs, HSCs, MSCs, pluripotent stem cells (PSCs, either embryonic stem cells-ESCs or induced PSCs-iPSCs), terminally differentiate into neuron-like cells after stimulation with nerve growth factor [54].

In order to restore the tissue function effectively, tissue engineered scaffolds should mimic the physical, chemical, and biological aspects of the native tissues. Peripheral nerves and spinal cords contain bundles of parallel axons myelinated by SCs and oligodendrocytes, respectively. Scaffolds with architectures in the longitudinal direction are supposed to provide contact guidance and regulate the orientation of growth and arrangement of the neurons [48]. Examples of such cues are imposed on patterned features, fibrous substrates, and hydrogel scaffolds, and their influence will be discussed in detail in the following sections. In addition, scaffold stiffness, degradability, and viscoelasticity are engineered to match native properties. For example, stiff networks may inhibit SC proliferation and elongation, as well as neurite extension [69,70]. The underlying mechanism is that mechanotransduction mismatches between the matrix and cells alter cellular phenotypes, proliferation, and differentiation ultimately [71]. Degradable scaffolds could facilitate intracellular signaling because they allow cells to be free to elongate or spread, benefiting further cellular responses and metabolic activities [72].

Axons transmit information through electrical impulses in the physiological state in the PNS and CNS. Electrical stimulation is another strategy for promoting nerve regeneration after injury [73]. The incorporation of electroconductive materials, like polypyrrole (PPY), into scaffolds not only increases pheochromocytoma cell proliferation but also accelerates axon myelination [74]. The density of newly regenerated axons was found to be much higher in conductive scaffolds [75]. The bioelectrical properties of cell membranes can generate weak electric fields locally, which, in turn, will be strengthened by conductive scaffolds to influence cell proliferation and differentiation under the mutual stimuli from adjacent cells [76].

Further, the introduction of neurotrophic factors to the scaffolds can also effectively promote cellular activities [48]. NGF, brain-derived neurotrophic factor (BDNF), neurotrophin 3/4/6 (NT-3/4/6), and glial cell line-derived neurotrophic factor (GDNF) are commonly used [77, 78]. These neurotrophic factors exert their actions through specific transmembrane receptors, like tropomyosin receptor kinase (Trk) and p75 [79], which activate a cascade of downstream signaling pathways to promote physiological neuron responses [80]. In this review, we focus on the anisotropic scaffolds and provide a detailed overview of fabrication, *in vitro* and *in vivo* efficacy, and potential mechanisms. The scaffolds in various spatial dimensions [i.e., surface patterns (1D plus), fibrous substrates (2D plus), and hydrogel (3D)] are mainly discussed.

### 3. Anisotropic surface patterns

Since P. Weiss introduced the term “contact guidance” in 1934 [81], many studies have benefited from elaborate techniques for fabricating 1D nano- and micro-patterned features for investigating the effects of topography on cellular reactions [82,83]. These patterns can be classified into continuous and discontinuous features [49]. Continuous topographies include grooves and ridges [84,85], while discontinuous ones include distributed pillars [86] and posts [87]. Many early studies hoped to address basic cellular responsive questions, while recent studies are focusing more on building nerve regeneration scaffolds with

**Table 1**

Cells used in peripheral nerve and spinal cord tissue engineering.

Cell type	Injury model	Source	Cell effects	Reference
Neural stem cell	SCI (monkey right-side C7 hemi-section); PNI (rat sciatic nerve crush)	Human embryonic spinal cord; induction from human ESCs	<ul style="list-style-type: none"> <li>● Axons from NSCs grow into host spinal cord</li> <li>● Form reciprocal synaptic connections with host circuits</li> <li>● Inhibit sciatic nerve inflammation</li> <li>● Promote sciatic nerve functional recovery</li> </ul>	[55,56]
Hematopoietic stem cell	SCI (rat T10 spinal cord complete transection); PNI (human patients)	Bone marrow	<ul style="list-style-type: none"> <li>● Promote oligogenesis and 5-HT fibers</li> <li>● Inhibit astrogliosis</li> <li>● Cause complications</li> </ul>	[57]
Mesenchymal stem cell	SCI (rat T9 spinal cord transection with 1.5 mm gap); PNI (rat sciatic nerve transection with 10 mm gap)	Bone marrow	<ul style="list-style-type: none"> <li>● Facilitate spinal cord integration</li> <li>● Inhibit glial scar formation and inflammatory cell infiltration</li> <li>● Provide favorable ECM for nerve regeneration</li> </ul>	[58–60]
Embryonic stem cell	SCI (mouse spinal cord compression); PNI (rat sciatic nerve transection with 10 mm gap)	Embryoid bodies	<ul style="list-style-type: none"> <li>● Rescue imperiled host motoneurons and parvalbumin-positive interneurons</li> <li>● Increase nerve fibers distal to the lesion</li> <li>● Enhanced expression and secretion of growth factors</li> <li>● Help axon regrowth</li> </ul>	[61,62]
Induced pluripotent stem cells	SCI (rat spinal cord contusion injury); PNI (5 mm gap in rat sciatic nerve)	Fetal lung fibroblasts; Cell line	<ul style="list-style-type: none"> <li>● Enhanced integration of neural lineage</li> <li>● Help axon regeneration and SCs maturation</li> </ul>	[63–66]
Schwann cells	SCI (patient chronic spinal cord injury); PNI (5 mm gap in rat sciatic nerve)	Sural nerve; Sciatic nerve	<ul style="list-style-type: none"> <li>● Generally safe for some patients</li> <li>● Help nerve axon regeneration and remyelination</li> </ul>	[67,68]
Astrocytes	SCI (1 mm spinal cord transection in rats)	Spinal cord	<ul style="list-style-type: none"> <li>● Promote recovery of volitional foot placement, axonal growth</li> </ul>	[52]

(continued on next page)

**Table 1** (continued)

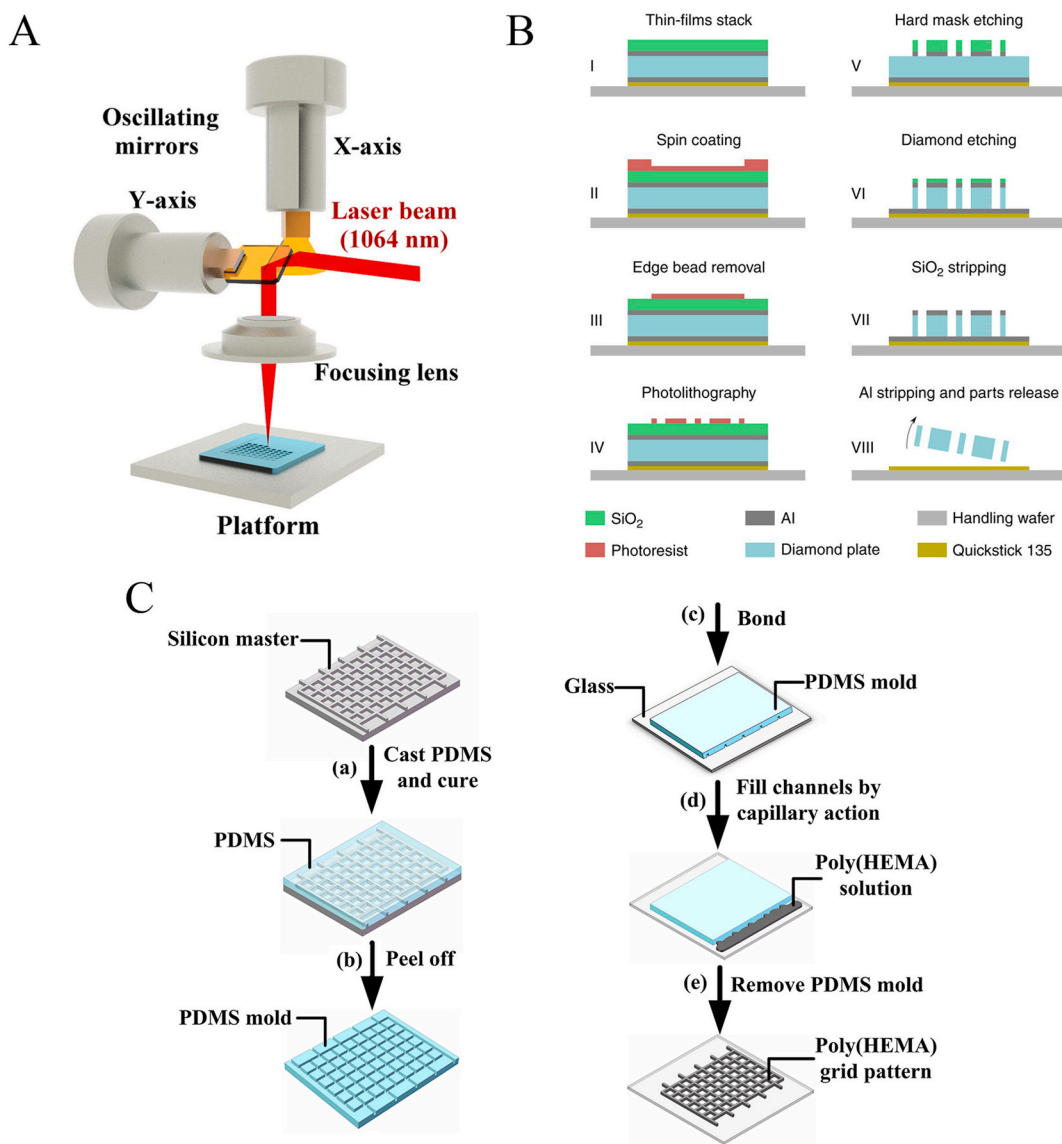
Cell type	Injury model	Source	Cell effects	Reference
Oligodendrocytes	SCI (rat spinal cord contusion injury)	Derived from rat ESCs	and neuronal survival ●Indicate conservation between rat and human ●Enhance axon remyelination ●Improve motor function	[53]

these patterned features [88].

**3.1. Fabrication methods and surface pattern strategies**

Silicon (Si), polystyrene (PS), and polydimethylsiloxane (PDMS) have been extensively utilized as nano- and micro-topographical substrates [89]. Degradable polymers, like poly (lactic acid) (PLA),

polycaprolactone (PCL), collagen, chitosan, and decellularized extracellular matrix, have also been used as substrates for *in vivo* nerve regeneration purpose [90–93]. In many cases, the substrates are immersed in the coating materials first, like collagen and poly-D-Lysine (PDL), to promote cell attachment [94]. Laser etching, photolithography, and soft lithography are three primary methods for patterning [95–98]. As shown in Fig. 3A, a laser provides a simple manufacturing process and complicated patterns without contact contamination. By altering the pulses, the depth of engraving or marking can be controlled. Photolithography uses ultraviolet (UV) or other lights to transfer a geometric pattern from a photomask to a photosensitive chemical photoresist on the Si substrate. The material under the exposure pattern is then etched or decomposed, while the material underneath the photoresist forms the desired pattern (Fig. 3B) [99]. Similar to photolithography, soft lithography constructs surface features through elastomeric molds, mostly PDMS (Fig. 3C) [100]. In addition, soft lithography techniques are cheap, fast, and precise. There are various techniques of soft lithography, including replica molding, microcontact printing, micromolding, and microtransferring [101]. Replica molding fabricates patterned surface by casting prepolymers onto PDMS stamps, while microcontact printing transfers a desired ink onto PDMS stamps



**Fig. 3.** A) Schematic of laser scanning [103]. Copyright 2018, Elsevier. B) Schematic of photolithography [99]. Copyright 2018, Springer Nature. C) Four major soft lithographic techniques [100]. Copyright 2015, AIP Publishing.

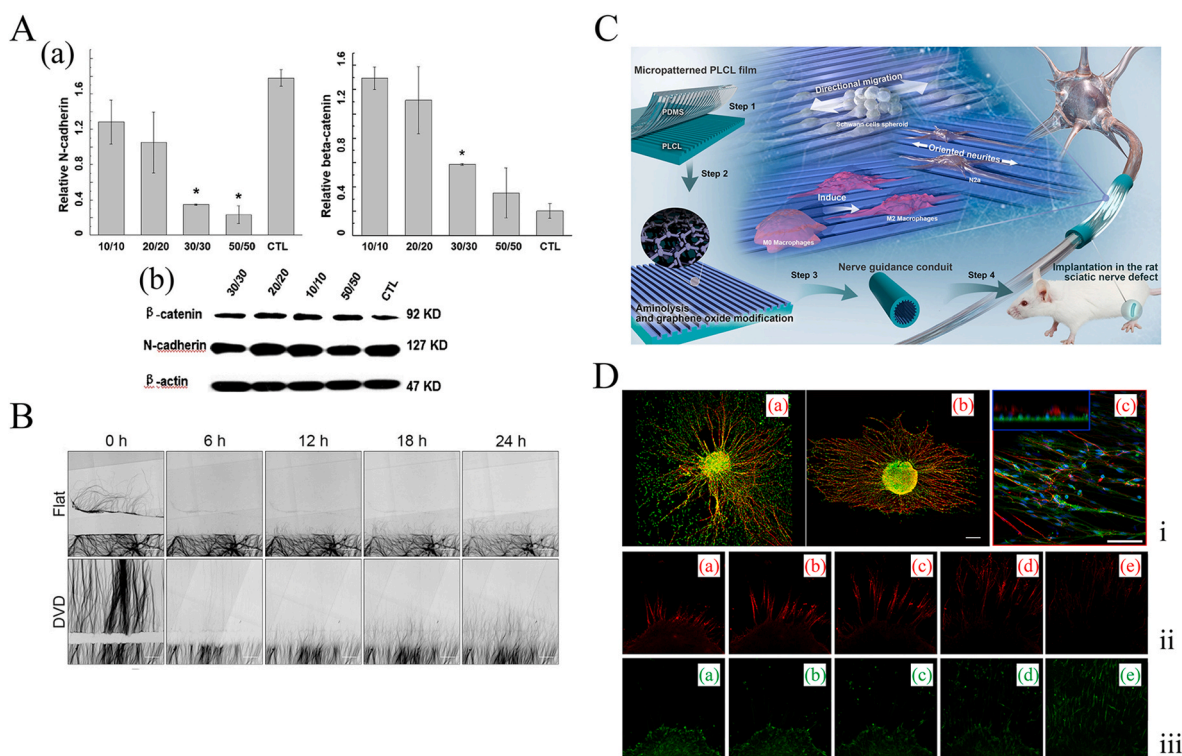
through direct contact with the substrate. PDMS serves as a negative mold after polymer casting and curing in micromolding and micro-transferring. Some studies also used nanoimprinting lithography to prepare grooves in nano size to direct axon growth [102].

### 3.2. Effects of patterned features on the behaviors of neural and glial cells

Topographical surfaces made from different materials have been systematically studied for their effects in neural and glial cell outgrowth. Grooves and ridges are the most studied continuous anisotropic geometries. The widths and depths of grooves are two critical parameters during designing. With regard to the depth, when increasing it in a broad range, from 0.2 to 69  $\mu\text{m}$ , more cells attached and proliferated along the groove direction [104]. In terms of the width, when approaching cellular size, cells not only grew more orientationally along the grooves but also significantly upregulated their genes related to regeneration and cytoskeletal development [48,105–109]. Li et al. fabricated groove patterns of four different sizes, with widths and depths of 10/10, 20/20, 30/30, and 50/50  $\mu\text{m}$ , respectively, on chitosan films by using micromolding. SCs randomly laid across the surface when the groove size (10/10  $\mu\text{m}$ ) was smaller than the cell size. However, for patterns with sizes (20/20  $\mu\text{m}$  and 30/30  $\mu\text{m}$ ) approaching the cell size (~20–30  $\mu\text{m}$ ), the seeded SCs aligned along the groove orientationally. By evaluating SC DNA synthesis, miRNA, and protein expression (N-cadherin and  $\beta$ -catenin) (Fig. 4A), it was demonstrated that this anisotropic topography could also up-regulate intracellular genes related to neuronal plasticity, axonal regeneration (smad6), cytoskeletal development

( $\beta$ -actin), and myelination (MPZ) [105]. During peripheral nerve regeneration, axons need to navigate to reach the distal segment, where Wallerian degeneration occurs. To match the diameter of axons (0.05–1.25  $\mu\text{m}$ ) without myelinating cells under injured conditions, Huang et al. used nanoimprinting to engineer parallel grooves on a poly (ethylene-co-vinyl acetate) (PEVA) copolymer surface [102]. Both peripheral neurons from DRG and cortical neurons survived and aligned within the grooves. To assess axon regeneration, axotomy experiments were performed on DRG seeded on a flat film and a  $905 \pm 6$  (pitch)/ $165 \pm 5$  (depth) nm film (named as DVD). As indicated in Fig. 4B, a grooved topography accelerated axon outgrowth to a greater degree than flat films.

In addition to regulating neuronal and glial cell behaviors *in vitro*, micropatterned films were also rolled into conduits and implanted *in vivo* [110–115]. For example, a 10 mm rat sciatic nerve gap was bridged by a nerve guidance conduit with grooves and graphene oxides in the inner wall (Fig. 4C). The conduit promoted nerve regeneration, indicated by the compound motor action potential (CMAP), nerve conduction velocity (NCV), wet weight of the gastrocnemius muscle, and positive S100 $\beta$  and NF200 area percentages, as well as the average myelinated axon diameter. These were comparable to those of the autograft group after 8 weeks [116]. Also, grooved nerve conduits were combined with microfibers to bridge a 10 mm sciatic nerve defect in rats. The micro-grooves on the inner surface promoted axonal outgrowth, while the inserted fibers could regulate cell orientation and migration. The composite scaffolds successfully re-bridged neurofilaments, and the sciatic function index, onset-to-peak of amplitude, and



**Fig. 4.** A) a: Protein expression levels of  $\beta$ -catenin and N-cadherin in Schwann cells on various micropatterned samples after 5 days of culture. b: Western blot images [105]. Copyright 2015, Elsevier. B) Time-lapse images of the DRG drop culture after on-site axotomy on flat (top) or DVD-spaced (bottom) surfaces. Axonal microtubules were stained with SiR-tubulin [102]. Copyright 2018, Wiley. C) Schematic of the fabrication of a PLCL film with micropatterns and its application for guiding nerve regeneration [116]. Copyright 2020, ACS Publications. D) i: Confocal microscopy images of whole DRG explants on low (a) and high (b) roughness micropatterned Si substrates. S100 positive Schwann cells and Neurofilament positive sympathetic neurons are labeled with green and red, respectively. Scale bar: 300  $\mu\text{m}$ . c: Confocal microscopy image of neurofilament positive sympathetic neurons (red), S100 positive Schwann cells (green), and TOPRO stained cell nuclei (blue) in a top view and xz optical section (inset). Scale bar: 75  $\mu\text{m}$  ii and iii: Spatial relationships between outgrown neurites and migrating Schwann cells emanating from a DRG explant positioned on medium roughness micropatterned Si substrates. Image sequence of confocal microscope optical sections of Neurofilament (NF) positive sympathetic neurons (red) (ii) and S100 positive Schwann cells (green) (iii). The different optical sections beginning from top (upper level of the DRG explant) to bottom (lower level of the Si substrate) are denoted as a to e, respectively [49]. Copyright 2015, Elsevier.

muscle weight were high after 8 weeks of implantation [115].

Apart from continuous grooves and ridges, where cells can grow and spread along with them [92,109,117,118], distributed pillars and posts can also form anisotropic structures to guide axon outgrowth [113, 119–121]. Simitzi et al. fabricated micro-cones on Si wafers using a pulsed laser [49]. Using a low energy laser, the surface was made to have an arbitrary shaped cross-section and arrangement of micro-cones. Through medium and high laser intensities, the resulting substrates presented elliptical micro-cones with preferential parallel alignment. The surface roughness and morphology significantly controlled axon outgrowth from rat sympathetic neurons and DRG. Neurons interacted with the upper part of the elliptical microcones and formed a tensed rope aligned along the direction of the parallelly oriented microcones, indicating a guidance effect of the underlying topography (Fig. 4D).

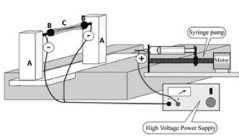

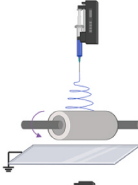

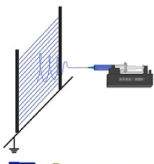
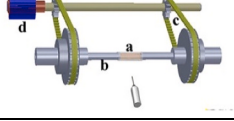
#### 4. Anisotropic fibrous scaffolds

Fibrous scaffolds have large surface area-to-volume ratios and porosities and are easy to process. Aligned fibers have been widely applied to mimic the anisotropic structures of axons in peripheral nerves and tracts in spinal cords [122–124]. Various natural and synthetic polymers can be utilized. Among various textile fabrication methods, electrospinning is the most promising approach for producing anisotropic fibrous substrates.

##### 4.1. Fabrication methods for anisotropic fibrous scaffolds

Electrospinning is the most commonly used method for fabricating aligned fibrous scaffolds for tissue engineering. Polymer solutions are drawn from the tip of a needle to a grounded collector by an electric field [125]. During this process, charged jets elongate and blend with each other and form nanofibers on the collector after solvent evaporation. A wide range of natural and synthetic polymers and their mixes can be applied to electrospinning. The solution needs to be conductive by either adopting polyelectrolytes or dissolving polymers in conductive solvents. Increasing the solution's conductivity can lower the initiating voltage of the electrospinning process and improve fiber quality by reducing beads [126]. Solution viscosity and solvent volatility also play important roles in electrospinning. It is difficult for electric charges to stretch highly viscous solutions, while polymers in low concentration cannot form continuous fibers [126]. Also, when charged jets travel from the needle tip to the collector, no fibers or fused fibers will be deposited on the collector if solvents evaporate slowly [126]. Through different collecting configurations, random or aligned fibrous scaffolds can be obtained [127]. For example, fibrous mats with randomly oriented fibers are collected on plates, while highly aligned ones can be collected on rotating drums, discs, wheels, etc. In Table 2, summaries of various collector sets with poles, discs, wheels, drums, and rods for fabricating aligned fibers in membranes, cylinders, or tubes are illustrated.

**Table 2**  
Collectors for aligned electrospinning fibrous nerve scaffolds.

Collectors	Illustration of the collector	Advantage	Disadvantage	Reference
Two pole air gap collectors		<ul style="list-style-type: none"> <li>● Aligned 3D cylindrical constructs</li> <li>● Easy to change scaffold void volume</li> </ul>	<ul style="list-style-type: none"> <li>● Alignment decreases when increase two pole distance</li> <li>● Tube collapse may happen</li> </ul>	[128], Copyright 2011, Elsevier.
Rotating disc collector		<ul style="list-style-type: none"> <li>● High alignment and productivity</li> </ul>	<ul style="list-style-type: none"> <li>● Complicated set-up</li> <li>● 2D fibrous membranes only</li> </ul>	[129]
Rotating drum collector		<ul style="list-style-type: none"> <li>● Simple set-up</li> <li>● Highly productive</li> </ul>	<ul style="list-style-type: none"> <li>● 2D fibrous membranes only</li> </ul>	[130]
Rotating wheel collector		<ul style="list-style-type: none"> <li>● Highly aligned</li> </ul>	<ul style="list-style-type: none"> <li>● Complicated set-up</li> <li>● Small fiber collection area</li> </ul>	[131]
Parallel electrode collector		<ul style="list-style-type: none"> <li>● Simple device</li> <li>● Large fiber collection area</li> </ul>	<ul style="list-style-type: none"> <li>● Less aligned when increasing electrode distance</li> <li>● 2D membrane only</li> </ul>	[132]
Rotating rods collector		<ul style="list-style-type: none"> <li>● Highly aligned fibrous cylinder</li> <li>● Prevent cylinder collapse</li> </ul>	<ul style="list-style-type: none"> <li>● Complicated set-up</li> <li>● Difficult to remove sample after fabrication</li> </ul>	[133], Copyright 2015, ACS Publications.

Although fiber diameter and alignment are easily controlled in electrospinning, the obtained scaffold has a small pore diameter, which inhibits cell penetration. In addition, nanofibrous constructs show limited mechanical performance. Therefore, many other fabrication methods, like self-assembly, wet phase inversion, phase separation, etc., are developed to further help nerve regeneration. Table 3 lists some fabrication techniques developed to produce aligned fibrous nerve scaffolds.

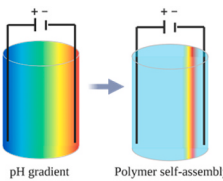
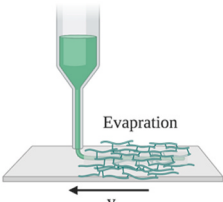
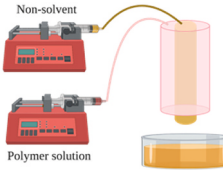
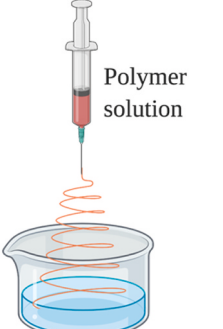
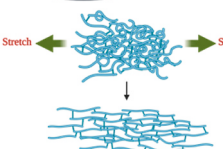
#### 4.2. Effects of aligned fibrous substrates on *in vitro* cell behaviors and *in vivo* efficacy

Neurons and glial cells can adhere to anisotropic fibrous scaffolds and elongate along the aligned fibers [121,130,139–146]. Chen et al. fabricated aligned gelatin methacryloyl (GelMA) fiber membranes and bundles for SCI treatment by using parallel electrode electrospinning collection [132]. They exhibited great viscoelasticity and fatigue resistance. Bone marrow derived MSCs (BMSCs) were seeded on fiber membranes, and the results demonstrated good biocompatibility as well as directional cellular adhesion and growth. Hippocampal neurons were also used to study the biological effects of the scaffolds, and the cells

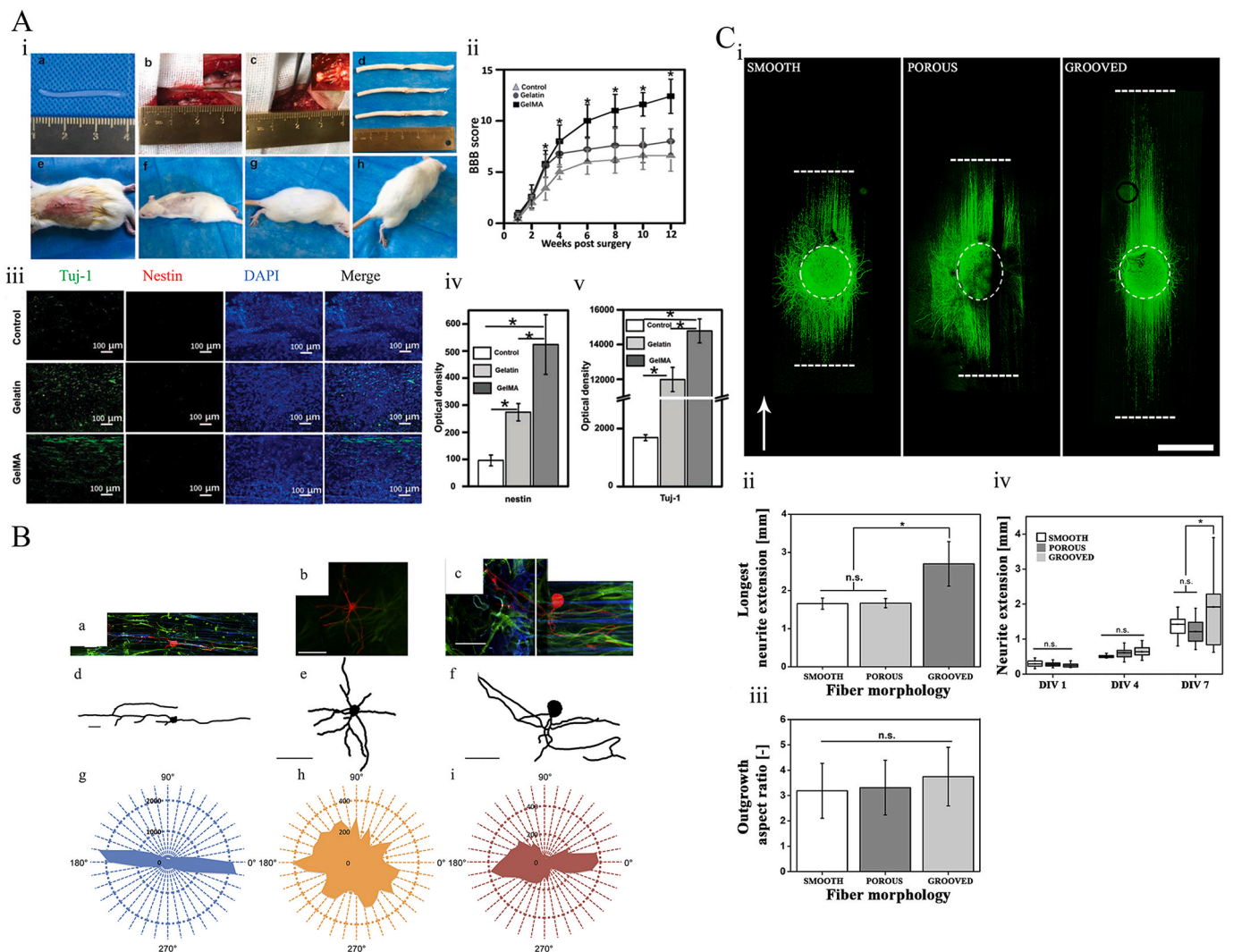
illustrated proliferation in the direction parallel to the long axis of the fibers. An SCI model was conducted on Sprague Dawley (SD) rats, and a 3 cm incision was made at the thoracic 9 vertebra (T9). GelMA groups promoted the recovery process after 12 weeks, according to the Basso, Beattie, and Bresnahan (BBB) locomotor rating scale. Ependymal cells, which are endogenous NSCs, differentiated into neurons and glial cells in the injured site. Immunohistochemical evaluation also illustrated higher nestin, Tuj-1, synaptophysin, and CD31 gene expressions in neurons after GelMA fiber implantation, compared to other groups (Fig. 5A). The presence of fewer astrocytes and glial scars confirmed that the GelMA fiber scaffolds promoted migration and differentiation of endogenous NSCs while suppressing glial scar formation. Aligned fibers were thought to induce the development of macrophage phenotypes that facilitate nerve regeneration. Nerve conduits were fabricated from aligned and random nanofibers, and the pro-healing macrophage ratio was higher in the aligned scaffolds during *in vivo* rat tests. Schwann cell infiltration and axon numbers were also higher in the aligned conduit group. It demonstrated that aligned fibers facilitated nerve regeneration, at least partly, by promoting the pro-healing macrophage phenotype [145].

Fibrous membranes with both anisotropic and isotropic regions were

**Table 3**  
Fabrication techniques to produce aligned fibrous nerve scaffolds.

Techniques	Schematic	Mechanism	Reference
Self-assembly		<ul style="list-style-type: none"> <li>Mainly for proteins (collagen, fibrin) with isoelectric points</li> <li>Protein solution under electrochemical reaction creates pH gradient and polymer precipitates</li> </ul>	[134]
Unidirectional shear force		<ul style="list-style-type: none"> <li>Polymers (fibronectin, collagen) form a liquid crystal-like solution in high concentration</li> <li>Orient along the force direction under unidirectional shear force</li> </ul>	[135]
Wet phase inversion		<ul style="list-style-type: none"> <li>Feasible for most polymers (PCL, PLA)</li> <li>By changing the flow rate ratio between polymer solution and its non-solvent, polymer precipitates with aligned grooves</li> </ul>	[136]
Phase separation		<ul style="list-style-type: none"> <li>Feasible for certain polymers (PCL, polyethylene oxide)</li> <li>Polymers go through phase changes when changing the environment of the solution</li> </ul>	[137]
Stretching		<ul style="list-style-type: none"> <li>Feasible for most polymers (collagen, cellulose)</li> <li>Orienting fibers through outside stretching forces</li> </ul>	[138]





**Fig. 5.** A) i: Pictures of animal experiments. a: Image of the electrospun GelMA hydrogel fiber scaffold. b: 3 mm hemisection made in the right site of the T9 spinal cord. c: Scaffold implantation. d: Spinal cord specimens collected 12 weeks after surgery. From top to bottom: control group, gelatin group, GelMA group. e–h: Animals at weeks 1, 4, 8, and 12 after surgery. ii: Evaluation of the lower limb motor function of rats with a BBB score. iii–v: Immunofluorescence staining of neural stem cells and neural cells and the quantitative comparison of the optical density among the groups. Samples without implants were used as a control group. \* $p < 0.05$  [132]. Copyright 2018, Wiley. B) a–c:  $40\times$  fluorescent images of individual neurons seeded on astrocytes, which were cultured on aligned fiber scaffolds (a), PLLA films (b), or fiber/AFFT scaffolds (c). d–f: Isolated traces of individual neurons pictured in a, b, and c, respectively. g–i: Polar histograms showing total outgrowth and orientation of neurites seeded on astrocyte layers, which were cultured on the three scaffold types (g = aligned fibers, h = film, i = AFFT boundary) [147]. Copyright 2015, Elsevier. C) DRG extension (green:  $\beta$  tubulin) on SAS fibers exhibiting smooth, porous, or grooved topographies (i). Grooved fibers demonstrate a significantly longer neurite extension compared to smooth and porous fibers after DIV 7 (ii). Effect of fiber surface topography on DRG surface area aspect ratio after DIV 7 (iii). Neurite extension length from DRGs on fibers after DIV 1, DIV 4, and DIV 7 (iv). Scale bar is 1 mm. The white arrow shows fiber direction [158]. Copyright 2020, Elsevier.

fabricated to compare their effects on cell behavior [147]. Highly aligned fibers were collected through rotating wheel using electrospinning, in which isotropic regions were created with nebulized chloroform. Astrocytes, as well as produced fibronectin and chondroitin sulfate proteoglycans (CSPGs), showed distinct morphological differences while growing on the aligned fibers and isotropic films. Astrocytes cultured on aligned fibers illustrated aligned tracts but showed disorganized ones on isotropic films. When neurites extended from the aligned fibers into the isotropic region, their orientation became less aligned or even stopped (Fig. 5B). The loss of neurite guidance is mostly due to astrocyte disorganization on isotropic films.

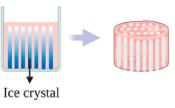
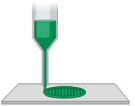
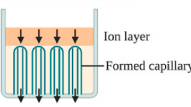
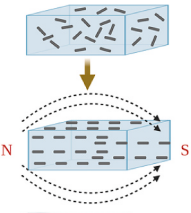
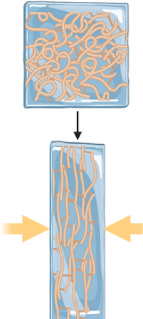
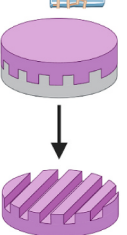
By introducing guidance cues from different scales (nano-scale to micro-scale), a higher percentage of neurite extension and function can be promoted [133,137,148,149]. Solvent assisted spinning was used to produce microfibers with smooth, grooved, and porous surface topographies, while the microfibers themselves were aligned at the microscale

level [148]. With the full DRG seeded, neurite extension on grooved fibers ( $2.3 \pm 0.4$  mm) was significantly longer compared to these seeded on smooth ( $1.6 \pm 0.5$  mm) and porous ( $1.7 \pm 0.4$  mm) fibers. Besides, DRG on grooved fibers were more aligned along the fiber direction (Fig. 5C). Grooved fibers also promoted a higher percentage of axon alignment growth from single neurons isolated from dissociated DRG.

## 5. Anisotropic 3D hydrogel scaffolds

Hydrogels are natural or polymeric 3D networks full of aqueous solutions. The 3D structures are similar to ECM and provide mechanical support for cell proliferation, while the water helps with nutritional diffusion. They have controllable flexibilities and porosities and are promising scaffolds for tissue engineering [150]. Hydrogels with anisotropic micro- or macro-structures can effectively induce aligned cellular growth and migration, which will accelerate tissue regeneration

**Table 4**  
Fabrication techniques to produce anisotropic hydrogel nerve scaffolds.

Technique	Illustration	Advantage	Disadvantage	Reference
Unidirectional freezing		<ul style="list-style-type: none"> <li>● Simple device</li> <li>● Applicable for almost all polymers</li> </ul>	<ul style="list-style-type: none"> <li>● Difficult to control the pore size</li> <li>● Cannot encapsulate cells</li> </ul>	[154]
3D printing		<ul style="list-style-type: none"> <li>● Create complicated structures</li> <li>● Cell encapsulation</li> </ul>	<ul style="list-style-type: none"> <li>● Many procedural steps</li> <li>● Expensive device</li> </ul>	[155]
Ion diffusion		<ul style="list-style-type: none"> <li>● Simple, without complicated device</li> </ul>	<ul style="list-style-type: none"> <li>● Applicable only to polymers reacting with ions</li> <li>● Difficult to control pore size</li> </ul>	[156]
Magnetic or electric field		<ul style="list-style-type: none"> <li>● Without contact contamination</li> </ul>	<ul style="list-style-type: none"> <li>● Magnetic or conductive materials added</li> </ul>	[157]
Stretching/compressing		<ul style="list-style-type: none"> <li>● Simple, without special device</li> <li>● Cell encapsulation</li> <li>● Feasible for most polymers</li> </ul>	<ul style="list-style-type: none"> <li>● May cause hydrogel breakage</li> <li>● Limited hydrogel shape</li> </ul>	[158]
Molding		<ul style="list-style-type: none"> <li>● Simple and applicable for most polymers</li> <li>● Cell encapsulation</li> </ul>	<ul style="list-style-type: none"> <li>● Need different molds for different shapes</li> </ul>	[159]

[151]. Studies have been exploring techniques to achieve anisotropic hydrogels for PNI and SCI treatment.

### 5.1. Fabrication strategies for anisotropic hydrogel scaffolds

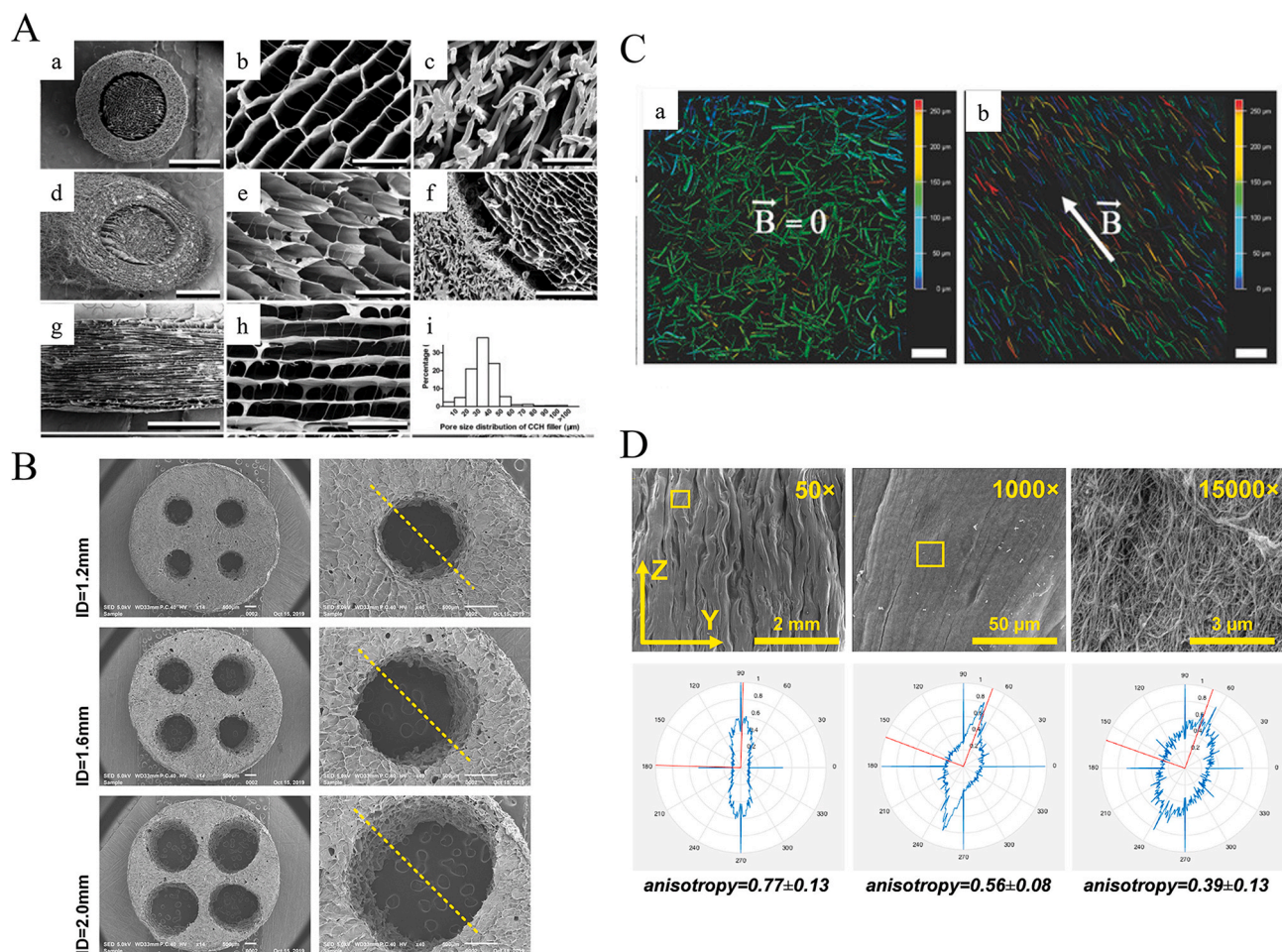
Various strategies have been applied to fabricate anisotropic hydrogels for axon regeneration (Table 4), including unidirectional freezing, 3D printing, ion diffusion, magnetic or electric field application, mechanical stretching, and molding [152,153].

Unidirectional freezing is simple and of wide application, suitable for polymer or monomer solutions and even decellularized nerve grafts [154,160–164]. Ice crystals grow inside the hydrogel along the uniaxial thermal gradient direction [165], forming parallel channels and pores after ice removal. A collagen/chitosan suspension was added into a polytetrafluoroethylene (PTFE) mold, whose bottom was sealed with a copper plate. The PTFE mold was then slowly moved towards the liquid nitrogen until completely immersed. The collagen/chitosan scaffold showed a honeycomb-like pattern in the transverse section with pore diameters in the range of 20  $\mu\text{m}$ –50  $\mu\text{m}$ . Longitudinal sections of the scaffold showed parallel, elongated microchannels (Fig. 6A) [162].

While unidirectional freezing hydrogels do not allow for

encapsulating cells inside, nor controlling the construct shape, 3D printing is a valuable technique for creating scaffolds with complex structures and cell encapsulation [166]. Software like Solidworks, AutoCAD, and Rhino can be used to help with the design. A fibrinogen solution combined with hyaluronic acid and polyvinyl alcohol was extruded to produce a hydrogel nerve regeneration scaffold [155]. The staining of fibrin showed aligned fibrin fibers parallel to the strand direction. The shear force during extrusion contributes to the rearrangement of fibrin fibers. Some static mixers are also adopted to endow hydrogels with internal anisotropic structures [167]. Besides, scaffolds with aligned micro-channels inside the hydrogel can be achieved directly through 3D printing (Fig. 6B) [168]. Silk fibroin is another promising natural biomaterial. It is nontoxic, nonimmunogenic, and FDA-approved [169]. Silk fibroin, together with many other biomaterials, has attracted a great deal of attention in the area of 3D printing nerve scaffolds [170]. However, a potential disadvantage of physically crosslinked silk fibroin hydrogels is that they are brittle, which makes them unable to undergo long range displacements and deformations [171].

Ion diffusion is also an easy method for forming anisotropic hydrogels with oriented channels, but it is limited to certain polymers that can



**Fig. 6.** A) SEM characterization of the scaffold. a–f: Transverse section of the scaffold (a, d) with collagen/chitosan filler (b, e) and PCL sheath (c, f). G–H: Longitudinal section of the collagen/chitosan filler. i: Pore size distribution of the collagen/chitosan filler. a, d, g: scale bars = 1 mm; b, c and e: scale bars = 50  $\mu\text{m}$ ; f: scale bar = 200  $\mu\text{m}$ ; h: scale bar = 100  $\mu\text{m}$  [162]. Copyright 2018, Elsevier. B) Scanning electron microscopy images of nerve guidance conduits showing the transverse section (dotted yellow line of the image on the right showing the plane where the samples were cut to acquire longitudinal images [181]). Copyright 2009, Elsevier. C) Depth color-coded images of magnetic fibers inside 3D fibrin hydrogels, prepared a: in the absence of an external magnetic field and b: in the presence of a 100 mT magnetic field [157]. Copyright 2017, Wiley. D) Multiscale anisotropy of biaxially compressed collagen scaffolds. The top row shows SEM images at the magnification specified in top right corner. The bottom row shows the corresponding polar plot from the image analysis, where the red lines represent the primary fiber axis, and the blue line is the magnitude of alignment at the specified angle [179]. Copyright 2018, Elsevier.

react with ions. Alginate is a chain-forming polysaccharide that can be gelled by many multivalent cations, like  $\text{Ca}^{2+}$ ,  $\text{Mg}^{2+}$ , and  $\text{Ba}^{2+}$ . By superimposing an aqueous solution containing multivalent cations in layers upon sodium alginate, a membrane boundary forms between the two liquids. Oriented diffusion of ions into sodium alginate causes continuous and layer-by-layer gel formation, leading to anisotropic capillary hydrogels [156,172–175]. After pouring ammonia onto the surface of a chitosan hydrogel with a low degree of crosslinking, ammonia permeates into the interior of the hydrogel by gravity. The discordance of the diffusion speed is caused by the high interior viscosity of the hydrogel and leads to ammonia accumulation and vacuoles, which become the seeds of the unidirectional structure [176]. A similar phenomenon was also demonstrated in poly (2,20-disulfonyl-4,40-benzidine terephthalamide) (PBTD) by cation diffusion [177].

Magnetic and electric fields are used as non-contacting external forces to rearrange hydrogel structures. For example, superparamagnetic iron oxide nanoparticles were added into microgels [178]. After treatment with a magnetic field, magnetoactive microgels were magnetized and arranged along the direction of the magnetic field. Then the surrounding hydrogel matrix was cross-linked *in situ* to keep the oriented microgel configuration (Fig. 6C) [157].

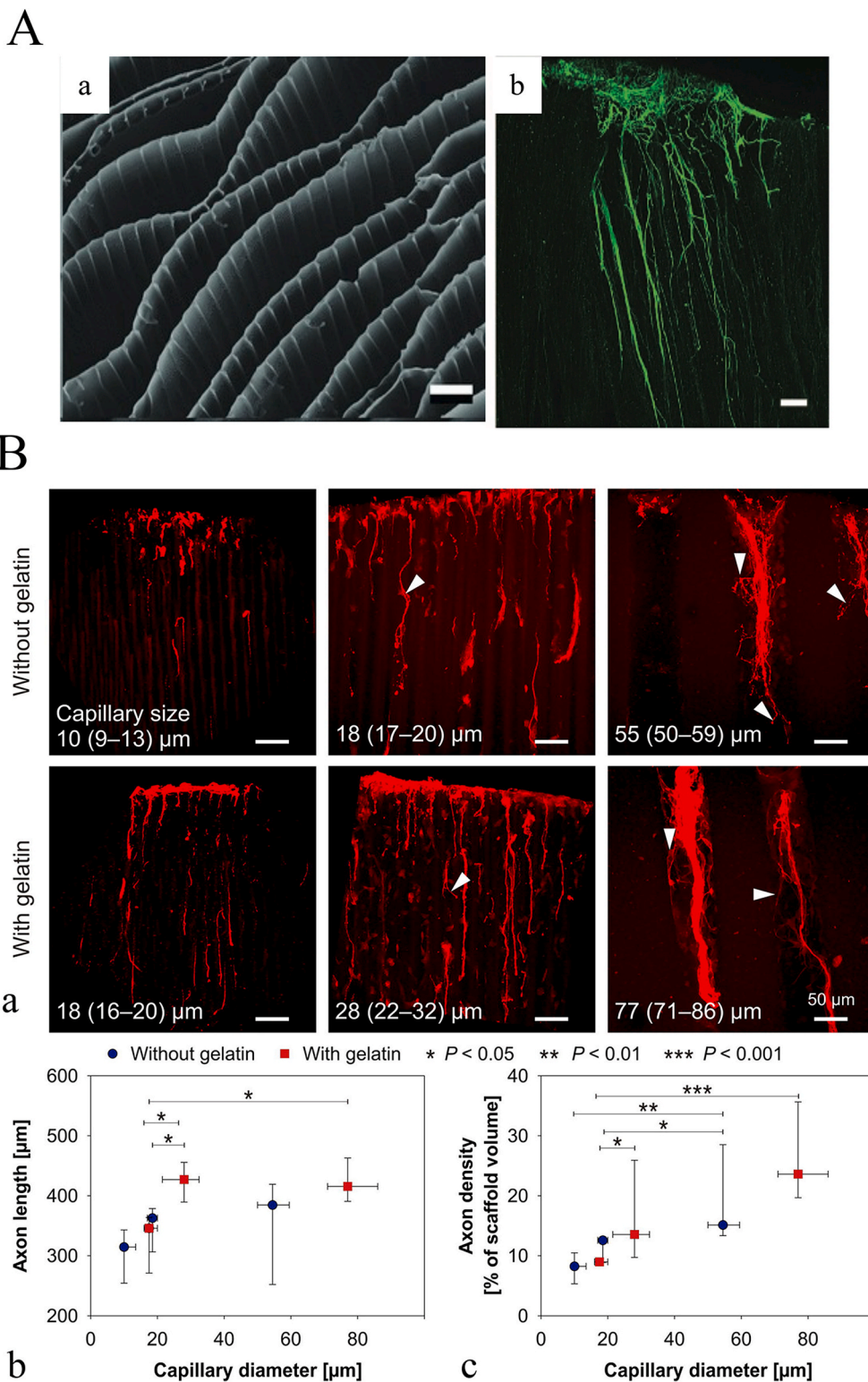
Under tensile or compressive strains, a cross-linked macromolecular

network reorder can be induced in prefabricated hydrogels (Fig. 6D) [179]. However, hydrogels are normally fragile, which limits their practical applications. Currently, some deformation-driven anisotropic hydrogels focus on nanofiber incorporation frameworks [158].

In addition, anisotropic hydrogel can also be fabricated through physical or chemical cue gradients, like growth factors [15,180]. A scaffold was created with four layers of gels from one end to the other, in which each layer contained a higher concentration of nerve growth factor than the previous layer, leading to step-gradient anisotropic scaffolds [180].

### 5.2. Effects of 3D anisotropic hydrogel scaffolds

Anisotropic hydrogel scaffolds with oriented pores or channels provide guidance cues for cells, affecting their growth direction and rate. Studies have shown that anisotropic hydrogels were advantageous for PNI and SCI treatment because they promote glial cell and axonal alignment, outgrowth, and myelination [182–187]. De Laporte and co-workers defined the term Anisogel, where a soft hydrogel surrounded magneto-responsive short fibers that were directionally oriented [157]. By mixing magnetic nanoparticles with poly (lactide-co-glycolide) (PLGA) in solution, short PLGA fibers were fabricated though

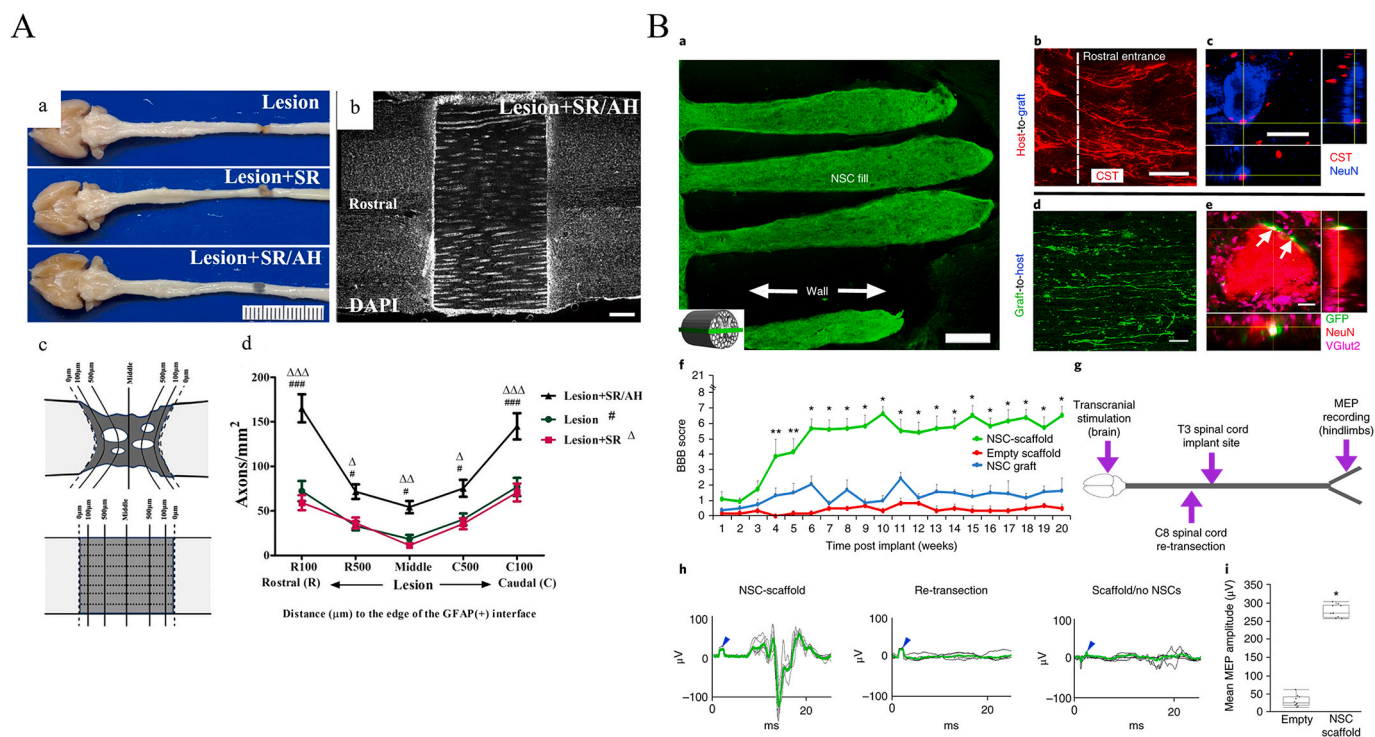


**Fig. 7.** A) SEM images of the scaffold with uniform ridges (a) and confocal microscopy of immunostained DRGs on the scaffold (b) [175]. Copyright 2012, Wiley. B) Axonal growth from DRGs into alginate with varying capillary sizes and densities. a: GAP-43-immunoreactive axons within Cu, Sr, and Zn hydrogels without (upper row) and with (lower row) gelatin. Quantification of (b) axon length and (c) axon density within various hydrogels. Arrowheads highlight examples of axon profiles deviating from the longitudinal capillary orientation. Scale bars are 50  $\mu\text{m}$  [173]. Copyright 2011, Elsevier.

electrospinning and microcutting processes. A low magnetic field was applied to the PLGA fibers and the fibrin precursor solution, and thus the PLGA fibers were oriented. In the case of DRGs encapsulated within hydrogels without fibers or with randomly oriented fibers, cells illustrated radial extension 55% and 34% lower than hydrogels with aligned fibers. Besides, an increase of cellular calcium levels in the Anisogel in the direction of the fibers further confirmed the cell alignment.

While it is difficult to control the structure inside anisotropic

hydrogels, the microstructure and size of aligned pores or channels does influence cellular orientation and axonal outgrowth velocity. Riblett et al. showed a chitosan scaffold with highly aligned pores and additional microridges to guide axons in multiple length scales for spinal cord regeneration [175]. The scaffolds were fabricated by carefully controlling unidirectional freezing, which gave aligned channels as the first features and uniform ridges parallel to the channels as secondary guidance features. Embryonic chicken DRGs shows excellent alignment



**Fig. 8.** A) a: Ventral view of chronic T5 transection sites of lesion, lesion + SR, and lesion + SR/AH animals. AHs fill the lesion and restore the continuity of the spinal cord. b: DAPI staining indicates that AHs integrated into the host parenchyma, and scaffold channels are filled with host cells. c: Schematic showing the virtual lines used to quantify βIII-tubulin labeled neurites. d: Quantification of neurites indicates more regrowth within the lesion in AH-grafted animals at all distances compared to nongrafted control subjects and a decrease in neurite number toward the center of the lesion (# $p < 0.05$ , ## $p < 0.001$  vs lesion group;  $\Delta p < 0.05$ ,  $\Delta\Delta p < 0.01$ ,  $\Delta\Delta\Delta p < 0.001$  vs lesion + SR group; \* $p < 0.05$ ; two-way ANOVA followed by Bonferroni post hoc test). Scale bar, a: 20 mm and b: 500  $\mu\text{m}$  [183]. Copyright 2020, ACS Publications. B) a: The channels are structurally intact and filled with GFP-expressing NPCs. The inset schematic diagram indicates the orientation of the horizontal sections in all panels of this figure, with rostral to the left. b: Corticospinal axons enter the scaffold and extend linearly in a caudal direction. c: CST axons converge on a NeuN-labeled neuron inside the channel, forming bouton-like contacts with the soma. d: GFP axons extend out from the scaffold into the host white and gray matter caudal to the lesion. Ventrolateral white matter, 2 mm caudal to the lesion. e: NPC-derived GFP-labeled axons form excitatory contacts (VGlut2) on host gray matter neurons (labeled for NeuN) located 2 mm caudal to the lesion (white arrows). f: BBB motor scores after complete transection (repeated-measures ANOVA; \*\* $P < 0.0232$ , \* $P < 0.0008$ ; mean  $\pm$  s.e.m.,  $n = 10$  animals). g: Schematic diagram of the electrophysiology study performed at 6 months post implantation. Transcranial electrical stimulation is applied to the motor cortex in the brain, and MEPs are recorded from the hindlimbs. h: Rats with 3D-printed, NPC-filled scaffolds exhibit MEP responses that are abolished by subsequent re-transection of the spinal cord immediately above the scaffold. Animals with empty scaffolds show no MEPs. The blue arrowheads mark stimulation artifacts. The green lines represent averages of several individual stimulations shown in black. i: The mean MEP amplitude is significantly greater in animals implanted with NPC-containing scaffolds. The boxes show the 25th–75th percentile range, and the center mark is the median. Whiskers show 1.5 times IQR from the 25th or 75th percentile values. (Student's t-test;  $P < 0.0001$ ,  $n = 10$  animals). Scale bars, 250  $\mu\text{m}$  (a), 50  $\mu\text{m}$  (b), 10  $\mu\text{m}$  (c), 40  $\mu\text{m}$  (d), and 5  $\mu\text{m}$  (e) [188]. Copyright 2019, Springer Nature.

within  $\pm 10^\circ$  of the channel direction (Fig. 7A). Pawar et al. fabricated alginate-based anisotropic hydrogels with capillary diameters of 10, 18, and 55  $\mu\text{m}$  by using  $\text{Cu}^{2+}$ ,  $\text{Sr}^{2+}$ , and  $\text{Zn}^{2+}$ , respectively [173]. After incorporating gelatin, the diameters of the capillaries became even wider. Neurites grew out from DRGs through the capillaries in the gels, and the length of axonal outgrowth was enhanced with wider capillary diameters, where axons also showed as bundles (Fig. 7B).

*In vivo* evaluations further confirmed the effects of anisotropic gel scaffolds. Alginate hydrogel (AH) scaffolds with longitudinal microchannels were fabricated by ion diffusion. A chronic thoracic (T5) transection model was performed on Fischer 344 rats [183]. Four weeks after the lesion, scaffolds were implanted into the thoracic cavity following scar resection (SR). The alginate scaffold completely filled the lesion and restored the integrity of the spinal cord after 12 weeks (Fig. 8A). Numerous host cells migrated across the entire hydrogel. Glial scarring was reduced in comparison with control animals without scaffold implantation. Biotinylated dextran amine (BDA)-labeled descending axons and cholera toxin  $\beta$ -subunit (CTB)-labeled ascending axons regenerated throughout the scaffolds and extended into the distal host parenchyma. Another scaffold with 200  $\mu\text{m}$  microchannels was printed by the microscale continuous projection method using polyethylene glycol–gelatin methacrylate (PEG–GelMA) [188]. Neural

progenitor cell (NPC) loaded scaffolds were implanted into rats that underwent T3 complete transections. After 4 weeks of implantation, NPCs completely filled the microchannels. Both axons derived from NPCs and host axons were in parallel linear arrays within channels, and many of them were myelinated by oligodendrocytes, as shown by ultrastructural images. After 6 months, the PEG–GelMA scaffolds degraded slowly. Host corticospinal axons entered the scaffold and extended linearly in a caudal direction. At the same time, NPC derived axons extended out of the scaffold into the host's spinal cord. Regarding the functional recovery, scaffolds with NPCs demonstrated significant improvement compared to empty scaffolds and mere NPCs, based on BBB motor scores and electrophysiological transmission (Fig. 8B).

Some anisotropic hydrogel scaffolds for nerve regeneration were based on aligned fibrous structures [146,189,190]. Topographical cues of fibers and soft, hydrophilic features of hydrogels were combined to better mimic axon structures. Oriented fibers induce neurite alignment and extension, while hydrogels protect nerve cells within the 3D architecture, which is promising for the biomimetic nerve regeneration scaffolds. Thus, they demonstrated an instructive microenvironment for accelerating axonal growth *in vivo* [191].

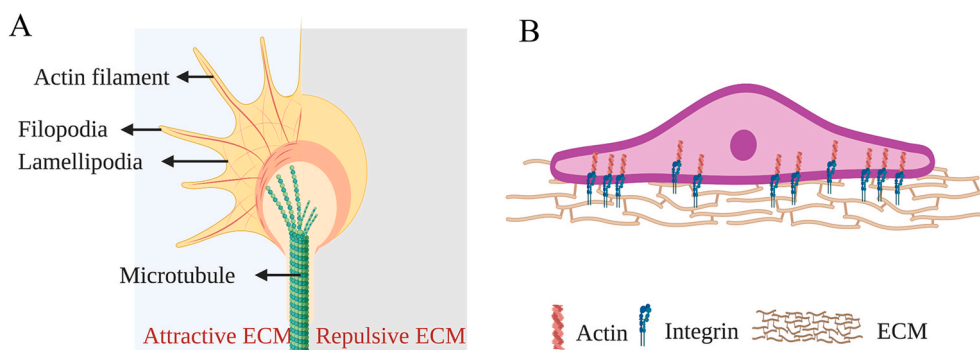


Fig. 9. Schematic of cellular response to ECM by the growth cone (A) and focal adhesion (B).

## 6. Mechanisms of neuron response to anisotropic structure and topography

The above sections highlight the fabrication technologies and approaches and the influence of obtained anisotropic features on neural and glial cell behaviors and nerve regeneration. The underlying mechanisms of neuronal response to topographic features remain to be clarified. Some hypotheses have been proposed and discussed explicitly in a previous review paper [192]. Here, we introduce the related theory from aspects of a growth cone and focal adhesion.

After PNI, SCs and macrophages remove inhibitory debris promptly, creating a beneficial environment for axon regrowth. And the Büngner bands, consisting of longitudinally oriented SCs, guide neurite extension through the growth cones [193]. Growth cones are the sensitive structures at the tips of growing axons, which consist of actin filaments and microtubules (Fig. 9A) [194]. These filaments and microtubules navigate growth cone behaviors, like advancing, retracting, turning, and branching, through receptors, such as netrins, slits, semaphorins, and ephrins [195]. The central region is bundled microtubules, and the periphery is dominated by a meshwork of lamellipodia and filopodia from actin filaments. Lamellipodia and filopodia greatly contribute to the sensing process. Filopodia are composed of bundles of filamentous F-actin, which can recognize morphology- and stress-associated cues. These actin filaments align with anisotropic cues to minimize cell cytoskeleton distortion or mechanical stress caused by the pattern [196–198]. The microtubules can grow and shrink dynamically, enabling them to explore lamellipodia and filopodia. Regulatory and structural interactions between actin and microtubules are essential for axon motility and growth cone guidance. The growth cone further interacts with myosin II motors and activates Yes-associated protein (YAP) [199], focal adhesion kinase (FAK) [200], integrin-linked kinase (ILK) [201], and tenascin-C (TN-C) [202], etc. as the axons grow. For example, YAP was found to be more activated and localized in neuronal nuclei when cultured on grooved surfaces than those on flat surfaces [199].

It is also widely accepted that integrin-based focal adhesion, which forms within extending filopodia or glial cell edges, also helps mediate neurite outgrowth along the ECM (Fig. 9B) [203]. Focal adhesions are made up of complex proteins that integrate the cell cytoskeleton with anisotropic substrates [204]. They stabilize filopodial extensions and turnovers quickly during growth cone movements [205]. The focal adhesion activates integrin binding. Integrins, which are transmembrane proteins, on the cell surface facilitate cell binding onto the substrates, causing gradual changes of bound cell morphology [204]. Proteomic techniques have been used to identify hundreds of adaptors and signaling proteins related to integrin adhesion, like paxillin, kindlin, and vinculin [206]. Paxillin is related to protrusion and is located at the cell periphery [207]. Vinculin has multiple functions and over 14 binding points [208]. Although neurons and glial cells can be guided through the growth cone and focal adhesion individually, they also have a complex interaction. At the beginning, SCs establish a pathway to

guide neuronal growth, and then neurons can grow past SCs afterwards, further guiding SC proliferation [209]. Besides neurons and glial cells, it has been demonstrated that an anisotropic topography could also help the development of regeneration promoting macrophage phenotypes [145]. The pro-healing macrophages, at least partly, facilitate the regeneration process.

Beyond the biochemical factors, topography may influence neurons and glial cell adhesion and growth via mechanobiology. It is suggested that surface roughness and topographical features may trigger mechanosensitive cellular ion channels, like the Piezo-1 [210]. Integrin is also thought to be the linker between topographical cues and cells. It has been shown that the migration of cells can be induced by shear stress [211]. Some intracellular signaling molecules, like Rho and Rac, have been indicated to be implicated in shear oriented migration [212]. It is hypothesized that the ability of cells to sense topographical cues is similar to their response to mechanical stimuli [192].

In addition to cell morphology, substrate topography can also influence biological functions of cells. Researchers evaluated the effects of anisotropic patterning on DNA synthesis, which is related to cell proliferation and differentiation [105]. They found that a micropatterning size that is similar to the cell size could activate a more vigorous DNA synthesis. Also, intracellular gene expression was affected. Genes related to cell adhesion, endocrine function, motility, and axon guidance were upgraded, while genes related to apoptosis, inflammation, and differentiation were downregulated [105]. It has been hypothesized that substrate topography may trigger a range of intracellular pathways to up- or down-regulate gene expressions [213]. The altered gene expressions further regulate protein expression and biological cell functions. Focal adhesion is thought to be the linker between topography and intracellular biological reactions [214]. It is able to change locations, compositions, and morphology along with the substrate topography [192]. Their exact relationship is not yet clear, and people are still working on figuring it out [215].

## 7. Conclusions and future prospects

Tissue engineering constructs are promising treatments for PNI and SCI [12]. They require biocompatible, biodegradable, porous scaffolds with appropriate mechanics and physical cues to promote axon regrowth. In this review, we focused on anisotropic scaffold fabrication for peripheral nerve and spinal cord regeneration, we reviewed how physical cues of anisotropy influence the regeneration efficacy. Three types of scaffolds were mainly discussed here: i) 2D patterned features, ii) fibrous substrates, and iii) hydrogel scaffolds. Lasers, photolithography, and soft lithography are mainly adopted to fabricate continuous and discontinuous features on 2D patterned surfaces. Studies have shown that micropatterned films help the alignment of neurons and glial cells, enhancing functional nerve recovery, and myelination. Electrospinning with multiple collectors is a major fabrication strategy for anisotropic fibrous scaffolds. Compared to randomly oriented fibers,

aligned fibrous mats or rolled tubes can direct cell reorganization along the long fiber axis. This further promotes axon or glial cell migration and regrowth. Anisotropic hydrogels with controlled porosities, oriented pores among the polymer structure as fabricated by unidirectional freezing or ion diffusion, and channels fabricated by 3D printing or molding hold great promise in peripheral nerve and spinal cord regeneration. One advantage of these hydrogels is their microscale sized pores, compared to the nanoscale pores of electrospinning fibrous scaffolds, which will not hinder cell infiltration. Another advantage is that hydrogels can engage cells and chemical molecules during fabrication to study the coordinated effects between topography and other cues. A lot of work regarding anisotropic peripheral nerve and spinal cord scaffold development has accelerated our understanding of nerve regeneration *in vitro* and *in vivo* [36,76,108], but how cells respond to these topographical cues at molecular and genetic levels remains to be answered. There is still a lack of clinically effective scaffolds. This may be due to inherent nerve complexities and a need for consideration of electrical stimulation, vascularization, and exogenous biochemical molecules [216–219].

Native axons are subject to cyclic electric impulses in order to transfer information. Therefore, appropriate electrical stimulation for cells encapsulated in the scaffolds and host neurons and glia is speculated to promote axon survival and migration [220,221]. Dong et al. incorporated graphene into electrospun fibrous scaffolds, and they found that electrical stimulation could accelerate cell migration and promote neurotrophic factor secretion *in vitro* as well as enhance sciatic nerve regeneration and functional recovery after implantation [222]. By including conductive materials, like gold nanoparticles, graphene, polyaniline, etc., we can combine an anisotropic topography with electrical stimulation to study their synergistic effects on nerve regeneration. One possible hurdle for bench to bedside translation may be the inconvenience of an exogenous electrical supply. Piezoelectric polyvinylidene fluoride (PVDF) nano/micro material incorporation can provide scaffolds with self-powered electrical stimulation [223,224]. The use of magnetic coupling can also achieve wireless power transfer in biofluids or tissues [225].

Vascularization is another compelling challenge and should be considered in the design of anisotropic nerve scaffolds. Vascularization ensures cellular survival by transporting nutrients and oxygen as well as supporting cellular metabolism and avoiding necrosis. Through encapsulating angiogenesis related growth factors, genes, and cells, a vascular network around axons could be achieved. The incorporation methods include physical embedding and surface immobilization. For example, a gene delivery system fabricated by polyethyleneimine was used to deliver plasmid DNA (pDNA) encoding vascular endothelial growth factor (VEGF), and regenerated microvessels in both peripheral nerves and gastrocnemius muscles can be seen after *in vivo* transfection [218]. Advanced 3D printing may also be able to print more precise scaffolds that can improve vascularization and further improve nerve graft survival and function. This is particularly important for SCI injury. The newly formed vessels after SCI initially lack a blood-spinal cord barrier (BSCB) [226]. The disruption of the BSCB function contributes to inflammation and reactive gliosis that inhibits axon growth and reconnection. Therefore, pre-vascularization of the scaffolds by using stem cells and delivery systems may improve BSCB integrity and thus reduce inflammation and scar formation at the injury site and improve axon growth [227,228]. The implementation of anisotropic scaffolds may further facilitate the integration process.

Biochemical molecular regulation of cell-ECM interaction (like NGF) and cell-cell interaction (such as cadherins and neural cell adhesion molecules) is another aspect we should pay attention to Ref. [229]. The practical consideration of biochemical molecular application is that they should be delivered to cells or injured nerves. To achieve this, those molecules can be coated onto or physical incorporated into anisotropic scaffolds [229]. Although it is simple, molecules may suffer from a short life. Chemical crosslinking and biochemical conjugation through IgG

antibodies are two main strategies for immobilizing them for long-term delivery [230,231]. Biomolecules can bind with IgG antibodies, and then Fc of IgG is conjugated chemically with scaffolds. In this way, biomolecules have a high immobilization rate as well as an undamaged bioactivity. Other techniques include local and long-term release from a functional biomaterial embedded in scaffolds. For example, a hollow, flower-shaped nano-ruthenium material was used as the NGF carrier and sealed with a phase change material. By increasing the temperature with near-infrared irradiation, the phase change material slowly melts and the nanocomposite can effectively release the NGF [232]. Through the cooperative functions of the anisotropic topography and biochemical cues, we can better mimic native nerves and accelerate regeneration after injury.

Many research studies have been conducted to help our understanding of the influencing factors for nerve regeneration and the requirements of nerve engineering scaffolds. They suggest that anisotropic constructs can promote axon regrowth and myelination. On one hand, we need to extend our understanding of the underlying mechanisms of how topographical cues affect cell behaviors. On the other hand, we can explore the combination of anisotropic topographical cues and other biophysical and biochemical cues, like electrical stimuli and bioactive molecules. Some relevant studies have demonstrated promising results regarding *in vitro* neuron oriented growth and *in vivo* nerve regeneration [160,233–236]. To make them transplantable from bench to bedside, a stable power supply and sustained local therapeutic agent release still require optimization.

#### Declaration of competing interest

The authors declare no conflict of interest.

#### Acknowledgement

We acknowledge support by a grant from the National Institute of General Medical Sciences, 1U54GM115458, and the UNMC Center for Heart and Vascular Research.

#### References

- [1] A.M. Sousa, K.A. Meyer, G. Santpere, F.O. Gulden, N. Sestan, Evolution of the human nervous system function, structure, and development, *Cell* 170 (2) (2017) 226–247.
- [2] P.A. Wieringa, A.R. Goncalves de Pinho, S. Micera, R.J. van Wezel, L. Moroni, Biomimetic architectures for peripheral nerve repair: a review of biofabrication strategies, *Advanced healthcare materials* 7 (8) (2018) 1701164.
- [3] N. Haan, B. Song, Therapeutic application of electric fields in the injured nervous system, *Adv. Wound Care* 3 (2) (2014) 156–165.
- [4] S. Baillieu, S. Chacaroun, S. Dautreleau, O. Detante, J. Pépin, S. Verges, Hypoxic conditioning and the central nervous system: a new therapeutic opportunity for brain and spinal cord injuries? *Exp. Biol. Med.* 242 (11) (2017) 1198–1206.
- [5] *Peripheral Nerve Injury and Current Treatment Strategies*. <https://www.intechopen.com/books/peripheral-nerve-regeneration-from-surgery-to-new-therapeutic-approaches-including-biomaterials-and-cell-based-therapies-development/peripheral-nerve-injury-and-current-treatment-strategies>, 2016.
- [6] *Neural Injury and Repair*. <https://medschool.ucsd.edu/som/neurosciences/research/interest-groups/Pages/neuronal-injury-repair.aspx>, 2020.
- [7] M.C. Dodla, M. Alvarado-Velez, V.J. Mukhatyar, R.V. Bellamkonda, Peripheral nerve regeneration, in: A. Atala, R. Lanza, A.G. Mikos, R. Nerem (Eds.), *Principles of Regenerative Medicine*, third ed., Academic Press, 2019, pp. 1223–1236.
- [8] F. May, A. Buchner, K. Matiasek, B. Schlenker, C. Stief, N. Weidner, Recovery of erectile function comparing autologous nerve grafts, unseeded conduits, Schwann-cell-seeded guidance tubes and GDNF-overexpressing Schwann cell grafts, *Disease models & mechanisms* 9 (12) (2016) 1507–1511.
- [9] A.K. Varma, A. Das, G. Wallace, J. Barry, A.A. Vertegel, S.K. Ray, N.L. Banik, Spinal cord injury: a review of current therapy, future treatments, and basic science frontiers, *Neurochem. Res.* 38 (5) (2013) 895–905.
- [10] B. Vignani, S. Rossi, G. Sandri, M.C. Bonferoni, F. Ferrari, Design and criteria of electrospun fibrous scaffolds for the treatment of spinal cord injury, *Neural regeneration research* 12 (11) (2017) 1786.
- [11] S. Jana, S.K.L. Levensgood, M. Zhang, Anisotropic materials for skeletal-muscle-tissue engineering, *Adv. Mater.* 28 (48) (2016) 10588–10612.
- [12] X. Gu, F. Ding, D.F. Williams, Neural tissue engineering options for peripheral nerve regeneration, *Biomaterials* 35 (24) (2014) 6143–6156.

- [13] X. Gu, F. Ding, Y. Yang, J. Liu, Construction of tissue engineered nerve grafts and their application in peripheral nerve regeneration, *Prog. Neurobiol.* 93 (2) (2011) 204–230.
- [14] Y. Wang, C. Zhou, M. Yao, Y. Li, Y. Liu, W. Zheng, Biodegradable parallel and porous HSPG/collagen scaffolds for the in vitro culture of NSCs for the spinal cord tissue engineering, *J. Porous Mater.* 19 (2) (2012) 173–180.
- [15] M.C. Dodla, R.V. Bellamkonda, Differences between the effect of anisotropic and isotropic laminin and nerve growth factor presenting scaffolds on nerve regeneration across long peripheral nerve gaps, *Biomaterials* 29 (1) (2008) 33–46.
- [16] L. Ning, H. Sun, T. Lelong, R. Guilloteau, N. Zhu, D.J. Schreyer, X. Chen, 3D bioprinting of scaffolds with living Schwann cells for potential nerve tissue engineering applications, *Biofabrication* 10 (3) (2018) 35014.
- [17] M. Georgiou, S.C. Bunting, H.A. Davies, A.J. Loughlin, J.P. Golding, J.B. Phillips, Engineered neural tissue for peripheral nerve repair, *Biomaterials* 34 (30) (2013) 7335–7343.
- [18] G. Gruener, J. Biller, Spinal cord anatomy, localization, and overview of spinal cord syndromes, *Continuum: Lifelong Learning in Neurology* vol. 14 (3) (2008) 11–35.
- [19] E. Diaz, H. Morales, Spinal cord anatomy and clinical syndromes, *Seminars in Ultrasound, CT and MRI* 37 (5) (2016) 360–371.
- [20] C.D. Etz, F.A. Kari, C.S. Mueller, D. Silovitz, R.M. Brenner, H.-M. Lin, R.B. Griep, The collateral network concept: a reassessment of the anatomy of spinal cord perfusion, *J. Thorac. Cardiovasc. Surg.* 141 (4) (2011) 1020–1028.
- [21] T.A. Cho, Spinal cord functional anatomy, *CONTINUUM: lifelong learning in neurology* 21 (1) (2015) 13–35.
- [22] **Spinal Cord.** <https://www.kenhub.com/en/library/anatomy/the-spinal-cord>, 2020.
- [23] H. Ellis, Anatomy of the spinal nerves and dermatomes, *Anaesth. Intensive Care Med.* 7 (11) (2006) 405–406.
- [24] A. Pujala, D. Blivis, M.J. O'Donovan, Interactions between dorsal and ventral root stimulation on the generation of locomotor-like activity in the neonatal mouse spinal cord, *Eneuro* 3 (3) (2016) 101–116.
- [25] P.A. Guertin, Central pattern generator for locomotion: anatomical, physiological, and pathophysiological considerations, *Front. Neurol.* 3 (2013) 183–198.
- [26] E. Than-Trong, L. Bally-Cuif, Radial glia and neural progenitors in the adult zebrafish central nervous system, *Glia* 63 (8) (2015) 1406–1428.
- [27] K.A. Langert, E.M. Brey, Strategies for targeted delivery to the peripheral nerve, *Front. Neurosci.* 12 (2018) 887–897.
- [28] C.A. Oyinbo, Secondary injury mechanisms in traumatic spinal cord injury: a nugget of this multiply cascade, *Acta Neurobiol. Exp.* 71 (2) (2011) 281–299.
- [29] C.S. Ahuja, J.R. Wilson, S. Nori, M.R. Kotter, C. Druschel, A. Curt, M.G. Fehlings, Traumatic spinal cord injury, *Nature reviews Disease primers* 3 (1) (2017) 1–21.
- [30] J. Wu, B.A. Stoica, A.I. Faden, Cell cycle activation and spinal cord injury, *Neurotherapeutics* 8 (2) (2011) 221–228.
- [31] S. Carelli, T. Giallongo, F. Rey, M. Colli, D. Tosi, G. Bulfamante, A.M. Di Giulio, A. Gorio, Neuroprotection, recovery of function and endogenous neurogenesis in traumatic spinal cord injury following transplantation of activated adipose tissue, *Cells* 8 (4) (2019) 329–353.
- [32] L.A. Simpson, J.J. Eng, J.T. Hsieh, D.L. Wolfe, The Spinal Cord Injury Rehabilitation Evidence Research Team, the health and life priorities of individuals with spinal cord injury: a systematic review, *J. Neurotrauma* 29 (8) (2012) 1548–1555.
- [33] A.D. Gaudet, P.G. Popovich, M.S. Ramer, Wallerian degeneration: gaining perspective on inflammatory events after peripheral nerve injury, *J. Neuroinflammation* 8 (1) (2011) 110–123.
- [34] L.S. Borges, S. Yechikhov, Y.I. Lee, J.B. Rudell, M.B. Friese, S.J. Burden, M. J. Ferns, Identification of a motif in the acetylcholine receptor  $\beta$  subunit whose phosphorylation regulates rapsyn association and postsynaptic receptor localization, *J. Neurosci.* 28 (45) (2008) 11468–11476.
- [35] P. Chen, X. Piao, P. Bonaldo, Role of macrophages in Wallerian degeneration and axonal regeneration after peripheral nerve injury, *Acta Neuropathol.* 130 (5) (2015) 605–618.
- [36] K. Jessen, R. Mirsky, The repair Schwann cell and its function in regenerating nerves, *J. Physiol.* 594 (13) (2016) 3521–3531.
- [37] G. Hussain, J. Wang, A. Rasul, H. Anwar, M. Qasim, S. Zafar, N. Aziz, A. Razaq, R. Hussain, J.L.G. de Aguilar, Current status of therapeutic approaches against peripheral nerve injuries: a detailed story from injury to recovery, *Int. J. Biol. Sci.* 16 (1) (2020) 116–134.
- [38] A.H. Tezcan, Peripheral nerve injury and current treatment strategies, books on demand, Croatia, 2017.
- [39] B.J. Pfister, T. Gordon, J.R. Loverde, A.S. Kochar, S.E. Mackinnon, D.K. Cullen, Biomedical engineering strategies for peripheral nerve repair: surgical applications, state of the art, and future challenges, *Crit. Rev. Biomed. Eng.* 39 (2) (2011) 81–124.
- [40] J.I. Leckenby, C. Furrer, L. Haug, B.J. Personeni, E. Vögelin, A retrospective case series reporting the outcomes of Avance nerve allografts in the treatment of peripheral nerve injuries, *Plast. Reconstr. Surg.* 145 (2) (2020) 368–381.
- [41] **AxoGen.** <https://www.axogeninc.com/avance-nerve-graft/>, 2020.
- [42] D. Arslantunali, T. Dursun, D. Yucel, N. Hasirci, V. Hasirci, Peripheral nerve conduits: technology update, *Medical Devices (Auckland, NZ)* 7 (2014) 405–424.
- [43] K. Venkatesh, S.K. Ghosh, M. Mullick, G. Manivasagam, D. Sen, Spinal cord injury: pathophysiology, treatment strategies, associated challenges, and future implications, *Cell Tissue Res.* 377 (2019) 125–151.
- [44] **National Institutes of Health.** <https://clinicaltrials.gov>, 2020.
- [45] A. Platt, B.T. David, Stem cell clinical trials in spinal cord injury: a brief review of studies in the United States, *Medicine* 7 (5) (2020) 27–36.
- [46] K. Venkatesh, S.K. Ghosh, M. Mullick, G. Manivasagam, D. Sen, Spinal cord injury: pathophysiology, treatment strategies, associated challenges, and future implications, *Cell Tissue Res.* 377 (2019) 125–151.
- [47] A.F. Sulong, N.H. Hassan, N.M. Hwei, Y. Lokanathan, A.S. Naicker, S. Abdullah, M.R. Yusof, O. Htwe, R. Idrus, N. Hafilah, Collagen-coated poly(lactic-glycolic acid) (PLGA) seeded with neural-differentiated human mesenchymal stem cells as a potential nerve conduit, *Adv. Clin. Exp. Med.* 23 (3) (2014) 353–362.
- [48] G. Li, X. Zhao, L. Zhang, C. Wang, Y. Shi, Y. Yang, Regulating Schwann cells growth by chitosan micropatterning for peripheral nerve regeneration in vitro, *Macromol. Biosci.* 14 (8) (2014) 1067–1075.
- [49] C. Simitzi, P. Efstathopoulos, A. Kourgiantaki, A. Ranella, I. Charalampopoulos, C. Fotakis, I. Athanassakis, E. Stratakis, A. Gravanis, Laser fabricated discontinuous anisotropic microconical substrates as a new model scaffold to control the directionality of neuronal network outgrowth, *Biomaterials* 67 (2015) 115–128.
- [50] Y. Dai, C.E. Hill, Transplantation of adult rat Schwann cells into the injured spinal cord, in: P. Monje, H. Kim (Eds.), *Schwann Cells*, Humana Press, New York, 2018, pp. 409–438.
- [51] L. Yang, Y. Ge, J. Tang, J. Yuan, D. Ge, H. Chen, H. Zhang, X. Cao, Schwann cells transplantation improves locomotor recovery in rat models with spinal cord injury: a systematic review and meta-analysis, *Cell. Physiol. Biochem.* 37 (6) (2015) 2171–2182.
- [52] S.J. Davies, C.H. Shih, M. Noble, M. Mayer-Proschel, J.E. Davies, C. Proschel, Transplantation of specific human astrocytes promotes functional recovery after spinal cord injury, *PLoS One* 6 (3) (2011), e17328.
- [53] J. Sharp, J. Frame, M. Siegenthaler, G. Nistor, H.S. Keirstead, Human embryonic stem cell-derived oligodendrocyte progenitor cell transplants improve recovery after cervical spinal cord injury, *Stem Cell.* 28 (1) (2010) 152–163.
- [54] C. Simitzi, E. Stratakis, C. Fotakis, I. Athanassakis, A. Ranella, Microconical silicon structures influence NGF-induced PCL2 cell morphology, *Journal of tissue engineering and regenerative medicine* 9 (4) (2015) 424–434.
- [55] E.S. Rosenzweig, J.H. Brock, P. Lu, H. Kumamaru, E.A. Salegio, K. Kadoya, J. L. Weber, J.J. Liang, R. Moseanko, S. Hawbecker, Restorative effects of human neural stem cell grafts on the primate spinal cord, *Nat. Med.* 24 (4) (2018) 484–490.
- [56] T. Chen, Y. Li, W. Ni, B. Tang, Y. Wei, J. Li, J. Yu, L. Zhang, J. Gao, J. Zhou, Human neural stem cell-conditioned medium inhibits inflammation in macrophages via Sirt-1 signaling pathway, *In Vitro and Promotes Sciatic Nerve Injury Recovery in Rats*, *Stem Cells and Development* 29 (16) (2020) 1084–1095.
- [57] L. Xiong, F. Liu, S. Deng, J. Liu, Q. Dan, P. Zhang, Y. Zou, Q. Xia, T. Wang, Transplantation of hematopoietic stem cells promotes functional improvement associated with NT-3-MEK-1 activation in spinal cord-transected rats, *Front. Cell. Neurosci.* 11 (2017) 213–226.
- [58] K.T. Wright, W.E. Masri, A. Osman, J. Chowdhury, W.E. Johnson, Concise review: bone marrow for the treatment of spinal cord injury: mechanisms and clinical applications, *Stem Cell.* 29 (2) (2011) 169–178.
- [59] L. Li, M. Han, X. Jiang, X. Yin, F. Chen, T. Zhang, H. Ren, J. Zhang, T. Hou, Z. Chen, Peptide-tethered hydrogel scaffold promotes recovery from spinal cord transection via synergism with mesenchymal stem cells, *ACS Appl. Mater. Interfaces* 9 (4) (2017) 3330–3342.
- [60] Y. Gu, Z. Li, J. Huang, H. Wang, X. Gu, J. Gu, Application of marrow mesenchymal stem cell-derived extracellular matrix in peripheral nerve tissue engineering, *Journal of Tissue Engineering and Regenerative Medicine* 11 (8) (2017) 2250–2260.
- [61] Y. Cui, J. Xu, G. Hargus, I. Jakovcevski, M. Schachner, C. Bernreuther, Embryonic stem cell-derived L1 overexpressing neural aggregates enhance recovery after spinal cord injury in mice, *PLoS One* 6 (3) (2011), e17126.
- [62] T. Ishii, E. Kawakami, K. Endo, H. Misawa, K. Watabe, Myelinating cocultures of rodent stem cell line-derived neurons and immortalized Schwann cells, *Neuropathology* 37 (5) (2017) 475–481.
- [63] S.E. Nutt, E. Chang, S.T. Suhr, L.O. Schlosser, S.E. Mondello, C.T. Moritz, J. B. Cibelli, P.J. Horner, Caudalized human iPSC-derived neural progenitor cells produce neurons and glia but fail to restore function in an early chronic spinal cord injury model, *Exp. Neurol.* 248 (2013) 491–503.
- [64] D. Qi, S. Wu, H. Lin, M.A. Kuss, Y. Lei, A. Krasnoslobodtsev, S. Ahmed, C. Zhang, H.J. Kim, P. Jiang, Establishment of a human iPSC-and nanofiber-based microphysiological blood-brain barrier system, *ACS Appl. Mater. Interfaces* 10 (26) (2018) 21825–21835.
- [65] W. Xu, C.S. Cox, Y. Li, Induced pluripotent stem cells for peripheral nerve regeneration, *J. Stem Cell* 6 (1) (2011) 39–49.
- [66] M. Ikeda, T. Uemura, K. Takamatsu, M. Okada, K. Kazuki, Y. Tabata, Y. Ikada, H. Nakamura, Acceleration of peripheral nerve regeneration using nerve conduits in combination with induced pluripotent stem cell technology and a basic fibroblast growth factor drug delivery system, *J. Biomedical Materials Research Part A* 102 (5) (2014) 1370–1378.
- [67] H. Saberi, P. Moshayedi, H.R. Aghayan, B. Arjmand, S.K. Hosseini, S.H. Emami-Razavi, V. Rahimi Movaghar, M. Raza, M. Firouzi, Treatment of chronic thoracic spinal cord injury patients with autologous Schwann cell transplantation: an interim report on safety considerations and possible outcomes, *Neurosci. Lett.* 443 (1) (2008) 46–50.
- [68] S. Wu, M. Kuss, D. Qi, J. Hong, H.-J. Wang, W. Zhang, S. Chen, S. Ni, B. Duan, Development of cryogel-based guidance conduit for peripheral nerve regeneration, *ACS Applied Bio Materials* 2 (11) (2019) 4864–4871.



- [69] S. Wang, D.H. Kempen, G.C. De Ruyter, L. Cai, R.J. Spinner, A.J. Windebank, M. J. Yaszemski, L. Lu, Molecularly engineered biodegradable polymer networks with a wide range of stiffness for bone and peripheral nerve regeneration, *Adv. Funct. Mater.* 25 (18) (2015) 2715–2724.
- [70] A. Balgude, X. Yu, A. Szymanski, R. Bellamkonda, Agarose gel stiffness determines rate of DRG neurite extension in 3D cultures, *Biomaterials* 22 (10) (2001) 1077–1084.
- [71] W. Ong, N. Marival, J. Lin, M.H. Nai, Y.S. Chong, C. Pinese, S. Sajikumar, C. T. Lim, C. Ffrench-Constant, M.E. Bechler, Biomimicking fiber platform with tunable stiffness to study mechanotransduction reveals stiffness enhances oligodendrocyte differentiation but impedes myelination through YAP-dependent regulation, *Small* 16 (37) (2020) 2003656.
- [72] C.M. Madl, B.L. LeSavage, R.E. Dewi, K.J. Lampe, S.C. Heilshorn, Matrix remodeling enhances the differentiation capacity of neural progenitor cells in 3D hydrogels, *Advanced Science* 6 (4) (2019) 1801716.
- [73] J. Du, G. Zhen, H. Chen, S. Zhang, L. Qing, X. Yang, G. Lee, H. Mao, X. Jia, Optimal electrical stimulation boosts stem cell therapy in nerve regeneration, *Biomaterials* 181 (2018) 347–359.
- [74] S. Wu, Y. Qi, W. Shi, M. Kuss, S. Chen, B. Duan, Electrospun conductive nanofiber yarns for accelerating mesenchymal stem cells differentiation and maturation into Schwann cell-like cells under a combination of electrical stimulation and chemical induction, *Acta Biomater.* (2020), <https://doi.org/10.1016/j.actbio.2020.11.042>. In press.
- [75] W. Jing, Q. Ao, L. Wang, Z. Huang, Q. Cai, G. Chen, X. Yang, W. Zhong, Constructing conductive conduit with conductive fibrous infilling for peripheral nerve regeneration, *Chem. Eng. J.* 345 (2018) 566–577.
- [76] R. Guo, S. Zhang, M. Xiao, F. Qian, Z. He, D. Li, X. Zhang, H. Li, X. Yang, M. Wang, Accelerating bioelectric functional development of neural stem cells by graphene coupling: implications for neural interfacing with conductive materials, *Biomaterials* 106 (2016) 193–204.
- [77] Z.A. Berrin, D. Burcu, A. Gamze, G.D. Ömür, Melatonin and sciatic nerve injury repair: a current perspective, *J. Neurorestoratol.* 6 (1) (2018) 49–60.
- [78] R.R. Sehgal, R. Banerjee, IKVAV-functionalized self-assembling peptide hydrogel for improved neural stem cell transplantation, *Nanomedicine* 8 (4) (2013) 521–522.
- [79] B.H. Norman, J.S. McDermott, Targeting the nerve growth factor (NGF) pathway in drug discovery. Potential applications to new therapies for chronic pain, *J. Medicinal Chemistry* 60 (1) (2017) 66–88.
- [80] L. Aloe, M.L. Rocco, P. Bianchi, L. Manni, Nerve growth factor: from the early discoveries to the potential clinical use, *J. Translational Medicine* 10 (1) (2012) 239–254.
- [81] P. Weiss, In vitro experiments on the factors determining the course of the outgrowing nerve fiber, *J. Exp. Zool.* 68 (3) (1934) 393–448.
- [82] A. Ferrari, M. Cecchini, A. Dhawan, S. Micera, I. Tonazzini, R. Stabile, D. Pignano, F. Beltram, Nanotopographic control of neuronal polarity, *Nano Lett.* 11 (2) (2011) 505–511.
- [83] V. Mellissinaki, A. Gill, I. Ortega, M. Vamvakaki, A. Ranella, J. Haycock, C. Fotakis, M. Farsari, F. Claeysens, Direct laser writing of 3D scaffolds for neural tissue engineering applications, *Biofabrication* 3 (4) (2011) 45005.
- [84] F. Johansson, P. Carlberg, N. Danielsen, L. Montelius, M. Kanje, Axonal outgrowth on nano-imprinted patterns, *Biomaterials* 27 (8) (2006) 1251–1258.
- [85] L. Yao, S. Wang, W. Cui, R. Sherlock, C. O'Connell, G. Damodaran, A. Gorman, A. Windebank, A. Pandit, Effect of functionalized micropatterned PLGA on guided neurite growth, *Acta Biomater.* 5 (2) (2009) 580–588.
- [86] M. Park, E. Oh, J. Seo, M.H. Kim, H. Cho, J.Y. Choi, H. Lee, I.S. Choi, Control over neurite directionality and neurite elongation on anisotropic micropillar arrays, *Small* 12 (9) (2016) 1148–1152.
- [87] J.N. Hanson, M.J. Motala, M.L. Heien, M. Gillette, J. Sweedler, R.G. Nuzzo, Textural guidance cues for controlling process outgrowth of mammalian neurons, *Lab Chip* 9 (1) (2009) 122–131.
- [88] S. Tawfik, M. De Volder, D. Copic, S.J. Park, C.R. Oliver, E.S. Polsen, M. J. Roberts, A.J. Hart, Engineering of micro- and nanostructured surfaces with anisotropic geometries and properties, *Adv. Mater.* 24 (13) (2012) 1628–1674.
- [89] F. Pan, M. Zhang, G. Wu, Y. Lai, B. Greber, H.R. Schöler, L. Chi, Topographic effect on human induced pluripotent stem cells differentiation towards neuronal lineage, *Biomaterials* 34 (33) (2013) 8131–8139.
- [90] E.M. Jeffries, Y. Wang, Biomimetic micropatterned multi-channel nerve guides by templated electrospinning, *Biotechnol. Bioeng.* 109 (6) (2012) 1571–1582.
- [91] H. Fujimaki, K. Uchida, G. Inoue, M. Miyagi, N. Nemoto, T. Saku, Y. Isobe, K. Inage, O. Matsushita, S. Yagishita, Oriented collagen tubes combined with basic fibroblast growth factor promote peripheral nerve regeneration in a 15 mm sciatic nerve defect rat model, *J. Biomed. Mater. Res.* 105 (1) (2017) 8–14.
- [92] G. Li, X. Zhao, W. Zhao, L. Zhang, C. Wang, M. Jiang, X. Gu, Y. Yang, Porous chitosan scaffolds with surface micropatterning and inner porosity and their effects on Schwann cells, *Biomaterials* 35 (30) (2014) 8503–8513.
- [93] F. Pati, J. Jang, D. Ha, S.W. Kim, J.W. Rhie, J.H. Shim, D.H. Kim, D.W. Cho, Printing three-dimensional tissue analogues with decellularized extracellular matrix bioink, *Nat. Commun.* 5 (1) (2014) 1–11.
- [94] S.J. Armstrong, M. Wiberg, G. Terenghi, P.J. Kingham, ECM molecules mediate both Schwann cell proliferation and activation to enhance neurite outgrowth, *Tissue Eng.* 13 (12) (2007) 2863–2870.
- [95] C.W. Yeh, L. Wang, H. Wu, Y.K. Hsieh, J. Wang, M. Chen, T. Wang, Development of biomimetic micro-patterned device incorporated with neurotrophic gradient and supportive Schwann cells for the applications in neural tissue engineering, *Biofabrication* 9 (1) (2017) 15024.
- [96] M. Sun, M. McGowan, P.J. Kingham, G. Terenghi, S. Downes, Novel thin-walled nerve conduit with microgrooved surface patterns for enhanced peripheral nerve repair, *J. Mater. Sci. Mater. Med.* 21 (10) (2010) 2765–2774.
- [97] B. Joddar, A.T. Guy, H. Kamiguchi, Y. Ito, Spatial gradients of chemotropic factors from immobilized patterns to guide axonal growth and regeneration, *Biomaterials* 34 (37) (2013) 9593–9601.
- [98] S. Zhang, S. Vijayavenkataraman, W.F. Lu, J.Y. Fuh, A review on the use of computational methods to characterize, design, and optimize tissue engineering scaffolds, with a potential in 3D printing fabrication, *J. Biomed. Mater. Res. B Appl. Biomater.* 107 (5) (2019) 1329–1351.
- [99] A. Toros, M. Kiss, T. Graziosi, H. Sattari, P. Gallo, N. Quack, Precision micro-mechanical components in single crystal diamond by deep reactive ion etching, *Microsystems & nanoengineering* 4 (1) (2018) 1–8.
- [100] F. Ye, J. Jiang, H. Chang, L. Xie, J. Deng, Z. Ma, W. Yuan, Improved single-cell culture achieved using micromolding in capillaries technology coupled with poly (HEMA), *Biomicrofluidics* 1 (4) (2015) 44106.
- [101] N.C. Lindquist, P. Nagpal, K.M. McPeak, D.J. Norris, S.H. Oh, Engineering metallic nanostructures for plasmonics and nanophotonics, *Rep. Prog. Phys.* 75 (3) (2012) 36501.
- [102] Y.A. Huang, C.T. Ho, Y.H. Lin, C.J. Lee, S.M. Ho, M.C. Li, E. Hwang, Nanoimprinted anisotropic topography preferentially guides axons and enhances nerve regeneration, *Macromol. Biosci.* 18 (12) (2018) 1800335.
- [103] E. Steck, H. Bertram, A. Walther, K. Brohm, B. Mroczek, M. Rathmann, C. Merle, M. Gelinsky, W. Richter, Enhanced biochemical and biomechanical properties of scaffolds generated by flock technology for cartilage tissue engineering, *Tissue Eng.* 16 (12) (2010) 3697–3707.
- [104] N. Li, A. Folch, Integration of topographical and biochemical cues by axons during growth on microfabricated 3-D substrates, *Exp. Cell Res.* 311 (2) (2005) 307–316.
- [105] G. Li, X. Zhao, L. Zhang, J. Yang, W. Cui, Y. Yang, H. Zhang, Anisotropic ridge/groove microstructure for regulating morphology and biological function of Schwann cells, *Applied Materials Today* 18 (2020) 100468.
- [106] M.J. Mahoney, R.R. Chen, J. Tan, W.M. Saltzman, The influence of microchannels on neurite growth and architecture, *Biomaterials* 26 (7) (2005) 771–778.
- [107] C.W. Li, B. Davis, J. Shea, H. Sant, B.K. Gale, J. Agarwal, Optimization of micropatterned poly (lactic-co-glycolic acid) films for enhancing dorsal root ganglion cell orientation and extension, *Neural regeneration research* 13 (1) (2018) 105–111.
- [108] I. Tonazzini, E. Jacchetti, S. Meucci, F. Beltram, M. Cecchini, Schwann cell contact guidance versus boundary interaction in functional wound healing along nano and microstructured membranes, *Advanced healthcare materials* 4 (12) (2015) 1849–1860.
- [109] D. Zhang, S. Wu, J. Feng, Y. Duan, D. Xing, C. Gao, Micropatterned biodegradable polyesters clicked with CQAASIKVAV promote cell alignment, directional migration, and neurite outgrowth, *Acta Biomater.* 74 (2018) 143–155.
- [110] Y.L. Lin, J.C. Jen, S. Hsu, M. Chiu, Sciatic nerve repair by microgrooved nerve conduits made of chitosan-gold nanocomposites, *Surg. Neurol.* 70 (2008) S9–S18.
- [111] S.H. Hsu, C.H. Su, I.M. Chiu, A novel approach to align adult neural stem cells on micropatterned conduits for peripheral nerve regeneration: a feasibility study, *Artif. Organs* 33 (1) (2009) 26–35.
- [112] A. Mobasser, A. Faroni, B.M. Minogue, S. Downes, G. Terenghi, A.J. Reid, Polymer scaffolds with preferential parallel grooves enhance nerve regeneration, *Tissue Eng.* 21 (5) (2015) 1152–1162.
- [113] G. Li, C. Xue, H. Wang, X. Yang, Y. Zhao, L. Zhang, Y. Yang, Spatially featured porous chitosan conduits with micropatterned inner wall and seamless sidewall for bridging peripheral nerve regeneration, *Carbohydr. Polym.* 194 (2018) 225–235.
- [114] H. Suo, Z. Wang, G. Dai, J. Fu, J. Yin, L. Chang, Polyacrylonitrile nerve conduits with inner longitudinal grooved textures to enhance neuron directional outgrowth, *Journal of Microelectromechanical Systems* 27 (3) (2018) 457–463.
- [115] J. Jeon, M.S. Lee, J. Lim, S. Park, S.M. Kim, D. Kim, G. Tae, H.S. Yang, Micro-grooved nerve guidance conduits combined with microfiber for rat sciatic nerve regeneration, *J. Ind. Eng. Chem.* 90 (2020) 214–223.
- [116] D. Zhang, Y. Yao, Y. Duan, X. Yu, H. Shi, J.R. Nakkala, X. Zuo, L. Hong, Z. Mao, C. Gao, Surface-anchored graphene oxide nanosheets on cell-scale micropatterned poly (d, l-lactide-co-caprolactone) conduits promote peripheral nerve regeneration, *ACS Appl. Mater. Interfaces* (7) (2020) 7915–7930.
- [117] M.R. Lee, K.W. Kwon, H. Jung, H.N. Kim, K.Y. Suh, K. Kim, K.S. Kim, Direct differentiation of human embryonic stem cells into selective neurons on nanoscale ridge/groove pattern arrays, *Biomaterials* 31 (15) (2010) 4360–4366.
- [118] S.E. Thomson, C. Charalambous, C.A. Smith, P.M. Tsimbouri, T. Déjardin, P. J. Kingham, A.M. Hart, M.O. Riehl, Microtopographical cues promote peripheral nerve regeneration via transient mTORC2 activation, *Acta Biomater.* 60 (2017) 220–231.
- [119] J. Veldhuizen, J. Cutts, D.A. Brafman, R.Q. Migrino, M. Nikkha, Engineering anisotropic human stem cell-derived three-dimensional cardiac tissue on-a-chip, *Biomaterials* 256 (2020) 120195.
- [120] T. Repić, K. Madirazza, E. Bektur, D. Sapunar, Characterization of dorsal root ganglion neurons cultured on silicon micro-pillar substrates, *Sci. Rep.* 6 (2016) 39560.
- [121] M. Mattotti, L. Micholt, D. Braeken, D. Kovacic, Characterization of spiral ganglion neurons cultured on silicon micro-pillar substrates for new auditory neuro-electronic interfaces, *J. Neural. Eng.* 12 (2) (2015) 26001.
- [122] R.V. Bellamkonda, Peripheral nerve regeneration: an opinion on channels, scaffolds and anisotropy, *Biomaterials* 27 (19) (2006) 3515–3518.

- [123] J. Silver, J.H. Miller, Regeneration beyond the glial scar, *Nat. Rev. Neurosci.* 5 (2) (2004) 146–156.
- [124] S. Wu, S. Ni, X. Jiang, M.A. Kuss, H. Wang, B. Duan, Guiding mesenchymal stem cells into myelinating schwann cell-like phenotypes by using electrospun core–sheath nanofibers, *ACS Biomater. Sci. Eng.* 5 (10) (2019) 5284–5294.
- [125] Z.M. Huang, Y.Z. Zhang, M. Kotaki, S. Ramakrishna, A review on polymer nanofibers by electrospinning and their applications in nanocomposites, *Compos. Sci. Technol.* 63 (15) (2003) 2223–2253.
- [126] J.M. Deitzel, J. Kleinmeyer, D. Harris, N.B. Tan, The effect of processing variables on the morphology of electrospun nanofibers and textiles, *Polymer* 42 (1) (2001) 261–272.
- [127] S.H. Park, M.S. Kim, B. Lee, J.H. Park, H.J. Lee, N.K. Lee, N.L. Jeon, K.-Y. Suh, Creation of a hybrid scaffold with dual configuration of aligned and random electrospun fibers, *ACS Appl. Mater. Interfaces* 8 (4) (2016) 2826–2832.
- [128] B.S. Jha, R.J. Colello, J.R. Bowman, S.A. Sell, K.D. Lee, J.W. Bigbee, G.L. Bowlin, W.N. Chow, B.E. Mathern, D.G. Simpson, Two pole air gap electrospinning: fabrication of highly aligned, three-dimensional scaffolds for nerve reconstruction, *Acta Biomater.* 7 (1) (2011) 203–215.
- [129] S.K. Vimal, N. Ahamad, D.S. Katti, A simple method for fabrication of electrospun fibers with controlled degree of alignment having potential for nerve regeneration applications, *Mater. Sci. Eng. C* 63 (2016) 616–627.
- [130] C. Wang, K. Zhang, C. Fan, X. Mo, H. Ruan, F. Li, Aligned natural–synthetic polyblend nanofibers for peripheral nerve regeneration, *Acta Biomater.* 7 (2) (2011) 634–643.
- [131] C.R. Wittmer, T. Claudepierre, M. Reber, P. Wiedemann, J.A. Garlick, D. Kaplan, C. Egles, Multifunctionalized electrospun silk fibers promote axon regeneration in the central nervous system, *Adv. Funct. Mater.* 21 (22) (2011) 4232–4242.
- [132] C. Chen, J. Tang, Y. Gu, L. Liu, X. Liu, L. Deng, C. Martins, B. Sarmento, W. Cui, L. Chen, Bioinspired hydrogel electrospun fibers for spinal cord regeneration, *Adv. Funct. Mater.* 29 (4) (2019) 1806899.
- [133] C. Huang, Y. Ouyang, H. Niu, N. He, Q. Ke, X. Jin, D. Li, J. Fang, W. Liu, C. Fan, Nerve guidance conduits from aligned nanofibers: improvement of nerve regeneration through longitudinal nanogrooves on a fiber surface, *ACS Appl. Mater. Interfaces* 7 (13) (2015) 7189–7196.
- [134] M.T. Abu Rub, K.L. Billiar, M.H. Van Es, A. Knight, B.J. Rodriguez, D.I. Zeugolis, S. McCMahon, A.J. Windebank, A. Pandit, Nano-textured self-assembled aligned collagen hydrogels promote directional neurite guidance and overcome inhibition by myelin associated glycoprotein, *Soft Matter* 7 (6) (2011) 2770–2781.
- [135] O.S. Ejim, G.W. Blunn, R.A. Brown, Production of artificial-orientated mats and strands from plasma fibronectin: a morphological study, *Biomaterials* 14 (10) (1993) 743–748.
- [136] N. Zhang, C. Zhang, X. Wen, Fabrication of semipermeable hollow fiber membranes with highly aligned texture for nerve guidance, *Journal of biomedical materials research Part A: an Official Journal of the Society for biomaterials, the Japanese Society for biomaterials, and the Australian Society for biomaterials and the Korean Society for biomaterials* 75 (4) (2005) 941–949.
- [137] Y. Chen, M.B. Taskin, Z. Zhang, Y. Su, X. Han, M. Chen, Bioadhesive anisotropic nanogrooved microfibers directing three-dimensional neurite extension, *Biomaterials science* 7 (5) (2019) 2165–2173.
- [138] S. Chen, C. Wu, A. Liu, D. Wei, Y. Xiao, Z. Guo, L. Chen, Y. Zhu, J. Sun, H. Luo, Biofabrication of nerve fibers with mimetic myelin sheath-like structure and aligned fibrous niche, *Biofabrication* 12 (3) (2020) 35013.
- [139] A. Cooper, N. Bhattarai, M. Zhang, Fabrication and cellular compatibility of aligned chitosan–PCL fibers for nerve tissue regeneration, *Carbohydr. Polym.* 85 (1) (2011) 149–156.
- [140] J.I. Kim, T.I. Hwang, L.E. Aguilar, C.H. Park, C.S. Kim, A controlled design of aligned and random nanofibers for 3D bi-functionalized nerve conduits fabricated via a novel electrospinning set-up, *Sci. Rep.* 6 (1) (2016) 1–12.
- [141] V. Cirillo, V. Guarino, M.A. Alvarez Perez, M. Marrese, L. Ambrosio, Optimization of fully aligned bioactive electrospun fibers for “in vitro” nerve guidance, *J. Mater. Sci. Mater. Med.* 25 (10) (2014) 2323–2332.
- [142] S.J. Lee, M. Heo, D. Lee, D.N. Heo, H.N. Lim, I.K. Kwon, Fabrication and design of bioactive agent coated, highly-aligned electrospun matrices for nerve tissue engineering: preparation, characterization and application, *Appl. Surf. Sci.* 424 (2017) 359–367.
- [143] M.F. Daud, K.C. Pawar, F. Claeysens, A.J. Ryan, J.W. Haycock, An aligned 3D neuronal–glial co-culture model for peripheral nerve studies, *Biomaterials* 33 (25) (2012) 5901–5913.
- [144] K. Zhang, H. Zheng, S. Liang, C. Gao, Aligned PLLA nanofibrous scaffolds coated with graphene oxide for promoting neural cell growth, *Acta Biomater.* 37 (2016) 131–142.
- [145] Y. Jia, W. Yang, K. Zhang, S. Qiu, J. Xu, C. Wang, Y. Chai, Nanofiber arrangement regulates peripheral nerve regeneration through differential modulation of macrophage phenotypes, *Acta Biomater.* 83 (2019) 291–301.
- [146] L. Wang, Y. Wu, T. Hu, P.X. Ma, B. Guo, Aligned conductive core-shell biomimetic scaffolds based on nanofiber yarns/hydrogel for enhanced 3D neurite outgrowth alignment and elongation, *Acta Biomater.* 96 (2019) 175–187.
- [147] J.M. Zuidema, G.P. Desmond, C.J. Rivet, K.R. Kearns, D.M. Thompson, R. J. Gilbert, Nebulized solvent ablation of aligned PLLA fibers for the study of neurite response to anisotropic-to-isotropic fiber/film transition (AFFT) boundaries in astrocyte–neuron co-cultures, *Biomaterials* 46 (2015) 82–94.
- [148] A. Omidinia-Anarkoli, J.W. Ephraim, R. Rimal, L. De Laporte, Hierarchical fibrous guiding cues at different scales influence linear neurite extension, *Acta Biomater.* 113 (2020) 350–359.
- [149] M. Liang, X. Chen, Y. Xu, L. Zhu, X. Jin, C. Huang, Double-grooved nanofiber surfaces with enhanced anisotropic hydrophobicity, *Nanoscale* 9 (42) (2017) 16214–16222.
- [150] R.Y. Tam, T. Fuehrmann, N. Mitrousis, M.S. Shoichet, Regenerative therapies for central nervous system diseases: a biomaterials approach, *Neuropsychopharmacology* 39 (1) (2014) 169–188.
- [151] G. Li, S. Li, L. Zhang, S. Chen, Z. Sun, S. Li, L. Zhang, Y. Yang, Construction of biofunctionalized anisotropic hydrogel micropatterns and their effect on schwann cell behavior in peripheral nerve regeneration, *ACS Appl. Mater. Interfaces* 11 (41) (2019) 37397–37410.
- [152] L. Yao, K.L. Billiar, A.J. Windebank, A. Pandit, Multichanneled collagen conduits for peripheral nerve regeneration: design, fabrication, and characterization, *Tissue Eng. C Methods* 16 (6) (2010) 1585–1596.
- [153] M. Zhu, W. Li, X. Dong, X. Yuan, A.C. Midgley, H. Chang, Y. Wang, H. Wang, K. Wang, P.X. Ma, In vivo engineered extracellular matrix scaffolds with instructive niches for oriented tissue regeneration, *Nat. Commun.* 10 (1) (2019) 1–14.
- [154] J. Wu, Y. Lin, J. Sun, Anisotropic volume change of poly (N-isopropylacrylamide)-based hydrogels with an aligned dual-network microstructure, *J. Mater. Chem.* 22 (34) (2012) 17449–17451.
- [155] S. England, A. Rajaram, D.J. Schreyer, X. Chen, Bioprinted fibrin-factor XIII-hyaluronate hydrogel scaffolds with encapsulated Schwann cells and their in vitro characterization for use in nerve regeneration, *Bioprinting* 5 (2017) 1–9.
- [156] P. Prang, R. Müller, A. Eljaouhari, K. Heckmann, W. Kunz, T. Weber, C. Faber, M. Vroemen, U. Bogdahn, N. Weidner, The promotion of oriented axonal regrowth in the injured spinal cord by alginate-based anisotropic capillary hydrogels, *Biomaterials* 27 (19) (2006) 3560–3569.
- [157] A. Omidinia-Anarkoli, S. Boesveld, U. Tuvshindorj, J.C. Rose, T. Haraszti, L. De Laporte, An injectable hybrid hydrogel with oriented short fibers induces unidirectional growth of functional nerve cells, *Small* 13 (36) (2017) 1702207.
- [158] D. Ye, Q. Cheng, Q. Zhang, Y. Wang, C. Chang, L. Li, H. Peng, L. Zhang, Deformation drives alignment of nanofibers in framework for inducing anisotropic cellulose hydrogels with high toughness, *ACS Appl. Mater. Interfaces* 9 (49) (2017) 43154–43162.
- [159] D. Neal, M.S. Sakar, L.S. Ong, H.H. Asada, Formation of elongated fascicle-inspired 3D tissues consisting of high-density, aligned cells using sacrificial outer molding, *Lab Chip* 14 (11) (2014) 1907–1916.
- [160] O.S. Manoukian, M.R. Arul, S. Rudraiah, I. Kalajzic, S.G. Kumbar, Aligned microchannel polymer-nanotube composites for peripheral nerve regeneration: small molecule drug delivery, *J. Contr. Release* 296 (2019) 54–67.
- [161] P. Divakar, K. Yin, U.G. Wegst, Anisotropic freeze-cast collagen scaffolds for tissue regeneration: how processing conditions affect structure and properties in the dry and fully hydrated states, *Journal of the mechanical behavior of biomedical materials* 90 (2019) 350–364.
- [162] L. Huang, L. Zhu, X. Shi, B. Xia, Z. Liu, S. Zhu, Y. Yang, T. Ma, P. Cheng, K. Luo, A compound scaffold with uniform longitudinally oriented guidance cues and a porous sheath promotes peripheral nerve regeneration in vivo., *Acta Biomater.* 68 (2018) 223–236.
- [163] L. Fan, J.L. Li, Z. Cai, X. Wang, Creating biomimetic anisotropic architectures with co-aligned nanofibers and macrochannels by manipulating ice crystallization, *ACS Nano* 12 (6) (2018) 5780–5790.
- [164] M. Chau, K.J. De France, B. Kopera, V.R. Machado, S. Rosenfeldt, L. Reyes, K. J. Chan, S. Förster, E.D. Cranston, T. Hoare, Composite hydrogels with tunable anisotropic morphologies and mechanical properties, *Chem. Mater.* 28 (10) (2016) 3406–3415.
- [165] M. Darder, P. Aranda, M.L. Ferrer, M.C. Gutiérrez, F. del Monte, E. Ruiz-Hitzky, Progress in bionanocomposite and bioinspired foams, *Adv. Mater.* 23 (44) (2011) 5262–5267.
- [166] C. Li, M. Kuss, Y. Kong, F. Nie, X. Liu, B. Liu, A. Dunaevsky, P. Fayad, B. Duan, X. Li, 3D printed hydrogels with aligned microchannels to guide neural stem cell migration, *ACS Biomater. Sci. Eng.* 7 (2021) 690–700.
- [167] M. Puertas Bartolomé, M.K. Włodarczy Biegun, A. Del Campo, B. Vázquez-Lasa, J. San Román, 3D printing of a reactive hydrogel bio-ink using a static mixing tool, *Polymers* 12 (9) (2020) 1986.
- [168] W. Ye, H. Li, K. Yu, C. Xie, P. Wang, Y. Zheng, P. Zhang, J. Xiu, Y. Yang, F. Zhang, 3D printing of gelatin methacrylate-based nerve guidance conduits with multiple channels, *Mater. Des.* 192 (2020) 108757.
- [169] L. Wei, S. Wu, M. Kuss, X. Jiang, R. Sun, P. Reid, X. Qin, B. Duan, 3D printing of silk fibroin-based hybrid scaffold treated with platelet rich plasma for bone tissue engineering, *Bioactive materials* 4 (2019) 256–260.
- [170] X. Yu, T. Zhang, Y. Li, 3D printing and bioprinting nerve conduits for neural tissue engineering, *Polymers* 12 (8) (2020) 1637.
- [171] C. Holland, K. Numata, J. Rnjak-Kovacina, F.P. Seib, The biomedical use of silk: past, present, future, *Advanced healthcare materials* 8 (1) (2019) 1800465.
- [172] J. Thumbs, H. Kohler, Capillaries in alginate gel as an example of dissipative structure formation, *Chem. Phys.* 208 (1) (1996) 9–24.
- [173] K. Pawar, R. Mueller, M. Caioni, P. Prang, U. Bogdahn, W. Kunz, N. Weidner, Increasing capillary diameter and the incorporation of gelatin enhance axon outgrowth in alginate-based anisotropic hydrogels, *Acta Biomater.* 7 (7) (2011) 2826–2834.
- [174] L. Huang, Y. Wang, M. Zhu, X. Wan, H. Zhang, T. Lei, A. Blesch, S. Liu, Anisotropic alginate hydrogels promote axonal growth across chronic spinal cord transections after scar removal, *ACS Biomater. Sci. Eng.* 6 (2020) 2274–2286.
- [175] B.W. Riblett, N.L. Francis, M.A. Wheatley, U.G. Wegst, Ice-templated scaffolds with microridged pores direct DRG neurite growth, *Adv. Funct. Mater.* 22 (23) (2012) 4920–4923.

- [176] X. Cai, L. Chen, T. Jiang, X. Shen, J. Hu, H. Tong, Facile synthesis of anisotropic porous chitosan/hydroxyapatite scaffolds for bone tissue engineering, *J. Mater. Chem.* 21 (32) (2011) 12015–12025.
- [177] W. Yang, H. Furukawa, J.P. Gong, Highly extensible double-network gels with self-assembling anisotropic structure, *Adv. Mater.* 20 (23) (2008) 4499–4503.
- [178] J.C. Rose, M. Cámara-Torres, K. Rahimi, J. Köhler, M. Möller, L. De Laporte, Nerve cells decide to orient inside an injectable hydrogel with minimal structural guidance, *Nano Lett.* 17 (6) (2017) 3782–3791.
- [179] J.L. Zitnay, S.P. Reese, G. Tran, N. Farhang, R.D. Bowles, J.A. Weiss, Fabrication of dense anisotropic collagen scaffolds using biaxial compression, *Acta Biomater.* 65 (2018) 76–87.
- [180] M.C. Dodla, R.V. Bellamkonda, Anisotropic scaffolds facilitate enhanced neurite extension in vitro, journal of biomedical materials research Part A: an official journal of the society for biomaterials, The Japanese Society for Biomaterials, and The Australian Society for Biomaterials and the Korean Society for Biomaterials 78 (2) (2006) 213–221.
- [181] L. De Laporte, Y. Yang, M.L. Zelvinyanskaya, B.J. Cummings, A.J. Anderson, L. D. Shea, Plasmid releasing multiple channel bridges for transgene expression after spinal cord injury, *Mol. Ther.* 17 (2) (2009) 318–326.
- [182] J.C. Rose, M.C. Torres, K. Rahimi, J. Köhler, M. Möller, L. De Laporte, Nerve cells decide to orient inside an injectable hydrogel with minimal structural guidance, *Nano Lett.* 17 (6) (2017) 3782–3791.
- [183] L. Huang, Y. Wang, M. Zhu, X. Wan, H. Zhang, T. Lei, A. Blesch, S. Liu, Anisotropic alginate hydrogels promote axonal growth across chronic spinal cord transections after scar removal, *ACS Biomater. Sci. Eng.* 6 (4) (2020) 2274–2286.
- [184] S. Yao, S. Yu, Z. Cao, Y. Yang, X. Yu, H. Mao, L. Wang, X. Sun, L. Zhao, X. Wang, Hierarchically aligned fibrin nanofiber hydrogel accelerated axonal regrowth and locomotor function recovery in rat spinal cord injury, *Int. J. Nanomed.* 13 (2018) 2883.
- [185] L. Wang, D. Song, X. Zhang, Z. Ding, X. Kong, Q. Lu, D.L. Kaplan, Silk–graphene hybrid hydrogels with multiple cues to induce nerve cell behavior, *ACS Biomater. Sci. Eng.* 5 (2) (2018) 613–622.
- [186] M.C. Echave, R.M. Dominguez, M. Gómez Florit, J.L. Pedraz, R.L. Reis, G. Orive, M.E. Gomes, Biphasic hydrogels integrating mineralized and anisotropic features for interfacial tissue engineering, *ACS Appl. Mater. Interfaces* 11 (51) (2019) 47771–47784.
- [187] T. Yu, L. Wen, J. He, Y. Xu, T. Li, W. Wang, Y. Ma, M.A. Ahmad, X. Tian, J. Fan, Fabrication and evaluation of an optimized acellular nerve allograft with multiple axial channels, *Acta Biomater.* 115 (2020) 235–249.
- [188] J. Koffler, W. Zhu, X. Qu, O. Platoshy, J.N. Dulin, J. Brock, L. Graham, P. Lu, J. Sakamoto, M. Marsala, Biomimetic 3D-printed scaffolds for spinal cord injury repair, *Nat. Med.* 25 (2) (2019) 263–269.
- [189] C. Wu, A. Liu, S. Chen, X. Zhang, L. Chen, Y. Zhu, Z. Xiao, J. Sun, H. Luo, H. Fan, Cell-laden electroconductive hydrogel simulating nerve matrix to deliver electrical cues and promote neurogenesis, *ACS Appl. Mater. Interfaces* 11 (25) (2019) 22152–22163.
- [190] C. Zheng, Z. Yang, S. Chen, F. Zhang, Z. Rao, C. Zhao, D. Quan, Y. Bai, J. Shen, Nanofibrous nerve guidance conduits decorated with decellularized matrix hydrogel facilitate peripheral nerve injury repair, *Theranostics* 11 (6) (2021) 2917–2931.
- [191] J. Du, J. Liu, S. Yao, H. Mao, J. Peng, X. Sun, Z. Cao, Y. Yang, B. Xiao, Y. Wang, Prompt peripheral nerve regeneration induced by a hierarchically aligned fibrin nanofiber hydrogel, *Acta Biomater.* 55 (2017) 296–309.
- [192] D. Hoffman Kim, J.A. Mitchell, R.V. Bellamkonda, Topography, cell response, and nerve regeneration, *Annu. Rev. Biomed. Eng.* 12 (2010) 203–231.
- [193] J.M. Stukel, R.K. Willits, Mechanotransduction of neural cells through cell–substrate interactions, *Tissue Eng. B Rev.* 22 (3) (2016) 173–182.
- [194] E.W. Dent, F. Tang, K. Kalil, Axon guidance by growth cones and branches: common cytoskeletal and signaling mechanisms, *Neuroscientist* 9 (5) (2003) 343–353.
- [195] K. Kalil, E.W. Dent, Touch and go: guidance cues signal to the growth cone cytoskeleton, *Curr. Opin. Neurobiol.* 15 (5) (2005) 521–526.
- [196] D.W. Hamilton, C. Oakley, N.A. Jaeger, D.M. Brunette, Directional change produced by perpendicularly-oriented microgrooves is microtubule-dependent for fibroblasts and epithelium, *Cell Motil Cytoskeleton* 66 (5) (2009) 260–271.
- [197] M.T. Frey, I.Y. Tsai, T.P. Russell, S.K. Hanks, Y. Wang, Cellular responses to substrate topography: role of myosin II and focal adhesion kinase, *Biophys. J.* 90 (10) (2006) 3774–3782.
- [198] X. Walboomers, H. Croes, L. Ginsel, J. Jansen, Growth behavior of fibroblasts on microgrooved polystyrene, *Biomaterials* 19 (20) (1998) 1861–1868.
- [199] I. Tonazzini, C. Masciullo, E. Savi, A. Sonato, F. Romanato, M. Cecchini, Neuronal contact guidance and Yap signaling on ultra-small nanogratings, *Sci. Rep.* 10 (1) (2020) 1–18.
- [200] M. Grove, P.J. Brophy, FAK is required for Schwann cell spreading on immature basal lamina to coordinate the radial sorting of peripheral axons with myelination, *J. Neurosci.* 34 (40) (2014) 13422–13434.
- [201] K. Fukuda, J.D. Knight, G. Piszczek, R. Kothary, J. Qin, Biochemical, proteomic, structural, and thermodynamic characterizations of integrin-linked kinase (ILK) CROSS-VALIDATION OF THE PSEUDOKINASE, *J. Biol. Chem.* 286 (24) (2011) 21886–21895.
- [202] M. Cheah, M.R. Andrews, Integrin activation: implications for axon regeneration, *Cells* 7 (3) (2018) 20.
- [203] Z. Wen, J.Q. Zheng, Directional guidance of nerve growth cones, *Curr. Opin. Neurobiol.* 16 (1) (2006) 52–58.
- [204] N.J. Sniadecki, R.A. Desai, S.A. Ruiz, C.S. Chen, Nanotechnology for cell–substrate interactions, *Ann. Biomed. Eng.* 34 (1) (2006) 59–74.
- [205] E. Robles, T.M. Gomez, Focal adhesion kinase signaling at sites of integrin-mediated adhesion controls axon pathfinding, *Nat. Neurosci.* 9 (10) (2006) 1274–1283.
- [206] E.R. Horton, A. Byron, J.A. Askari, D.H. Ng, A. Millon-Frémillon, J. Robertson, E. J. Koper, N.R. Paul, S. Warwood, D. Knight, Definition of a consensus integrin adhesome and its dynamics during adhesion complex assembly and disassembly, *Nat. Cell Biol.* 17 (12) (2015) 1577–1587.
- [207] R.Z. Bar, R. Milo, Z. Kam, B. Geiger, A paxillin tyrosine phosphorylation switch regulates the assembly and form of cell–matrix adhesions, *J. Cell Sci.* 120 (1) (2007) 137–148.
- [208] P. Atherton, B. Stutchbury, D. Wang, D. Jethwa, R. Tsang, E.M. Rodriguez, P. Wang, N. Bate, R. Zent, I.L. Barsukov, Vinculin controls talin engagement with the actomyosin machinery, *Nat. Commun.* 6 (1) (2015) 1–12.
- [209] X. Wen, P.A. Tresco, Effect of filament diameter and extracellular matrix molecule precoating on neurite outgrowth and Schwann cell behavior on multifilament entubulation bridging device in vitro, *J. Biomed. Mater. Res. Part A: An Official Journal of The Society for Biomaterials, The Japanese Society for Biomaterials, and The Australian Society for Biomaterials and the Korean Society for Biomaterials* 76 (3) (2006) 626–637.
- [210] C. Simitzi, A. Ranella, E. Stratakis, Controlling the morphology and outgrowth of nerve and neuroglial cells: the effect of surface topography, *Acta Biomater.* 51 (2017) 21–52.
- [211] S. Li, N.F. Huang, S. Hsu, Mechanotransduction in endothelial cell migration, *J. Cell. Biochem.* 96 (6) (2005) 1110–1126.
- [212] B.W. Stothard, A.J. Ridley, Shear stress-induced endothelial cell polarization is mediated by Rho and Rac but not Cdc42 or PI 3-kinases, *J. Cell Biol.* 161 (2) (2003) 429–439.
- [213] K.N. Dahl, A.J. Ribeiro, J. Lammerding, Nuclear shape, mechanics, and mechanotransduction, *Circ. Res.* 102 (11) (2008) 1307–1318.
- [214] M. Chiquet, L. Gelman, R. Lutz, S. Maier, From mechanotransduction to extracellular matrix gene expression in fibroblasts, *Biochim. Biophys. Acta Mol. Cell Res.* 1793 (5) (2009) 911–920.
- [215] S. Cho, A.K. Muthukumar, T. Stork, J.C. Coutinho-Budd, M.R. Freeman, Focal adhesion molecules regulate astrocyte morphology and glutamate transporters to suppress seizure-like behavior, *Proc. Natl. Acad. Sci. Unit. States Am.* 115 (44) (2018) 11316–11321.
- [216] C. Wang, Y. Jia, W. Yang, C. Zhang, K. Zhang, Y. Chai, Silk fibroin enhances peripheral nerve regeneration by improving vascularization within nerve conduits, *J. Biomed. Mater. Res.* 106 (7) (2018) 2070–2077.
- [217] R. Li, D. Li, C. Wu, L. Ye, Y. Wu, Y. Yuan, S. Yang, L. Xie, Y. Mao, T. Jiang, Nerve growth factor activates autophagy in Schwann cells to enhance myelin debris clearance and to expedite nerve regeneration, *Theranostics* 10 (4) (2020) 1649.
- [218] Z. Fang, X. Ge, X. Chen, Y. Xu, W. Yuan, Y. Ouyang, Enhancement of sciatic nerve regeneration with dual delivery of vascular endothelial growth factor and nerve growth factor genes, *J. Nanobiotechnol.* 18 (1) (2020) 1–14.
- [219] K.J. Zuo, T. Gordon, K.M. Chan, G.H. Borschel, Electrical stimulation to enhance peripheral nerve regeneration: update in molecular investigations and clinical translation, *Exp. Neurol.* 332 (2020) 113397.
- [220] H.J. Kim, J.S. Lee, J.M. Park, S. Lee, S.J. Hong, J.S. Park, K. Park, Fabrication of nanocomposites complexed with gold nanoparticles on polyaniline and application to their nerve regeneration, *ACS Appl. Mater. Interfaces* 12 (27) (2020) 30750–30760.
- [221] J.L. Senger, K.N. Rabey, M.J. Morhart, K.M. Chan, C.A. Webber, Conditioning electrical stimulation accelerates regeneration in nerve transfers, *Ann. Neurol.* 8 (2020) 363–374.
- [222] C. Dong, F. Qiao, W. Hou, L. Yang, Y. Lv, Graphene-based conductive fibrous scaffold boosts sciatic nerve regeneration and functional recovery upon electrical stimulation, *Applied Materials Today* 21 (2020) 100870.
- [223] Y. Cheng, Y. Xu, Y. Qian, X. Chen, Y. Ouyang, W. Yuan, 3D structured self-powered PVDF/PCL scaffolds for peripheral nerve regeneration, *Nanomater. Energy* 69 (2020) 104411.
- [224] M. Mohseni, A.R. SA, F.H. Shirazi, N.H. Nemati, Preparation and characterization of self-electrical stimuli conductive gelatin based nano scaffold for nerve regeneration containing chopped short spun nanofibers of PVDF/MCM41 and polyaniline/graphene nanoparticles: physical, mechanical and morphological studies, *Int. J. Biol. Macromol.* 167 (2020) 887–893.
- [225] Y.S. Choi, Y. Hsueh, J. Koo, Q. Yang, R. Avila, B. Hu, Z. Xie, G. Lee, Z. Ning, C. Liu, Stretchable, dynamic covalent polymers for soft, long-lived bioresorbable electronic stimulators designed to facilitate neuromuscular regeneration, *Nat. Commun.* 11 (1) (2020) 1–14.
- [226] S.A. Fingle, R. Khosravi, J.M. Legasto, Y. Tseng, M.G. Fehlings, Characterization of vascular disruption and blood–spinal cord barrier permeability following traumatic spinal cord injury, *J. Neurotrauma* 31 (6) (2014) 541–552.
- [227] S. Guo, I. Redenski, S. Landau, A. Szklanny, U. Merdler, S. Levenberg, Prevascularized scaffolds bearing human dental pulp stem cells for treating complete spinal cord injury, *Advanced Healthcare Materials* 9 (20) (2020) 2000974.
- [228] K.A. Tran, P.P. Partyka, Y. Jin, J. Bouyer, I. Fischer, P.A. Galie, Vascularization of self-assembled peptide scaffolds for spinal cord injury repair, *Acta Biomater.* 104 (2020) 76–84.
- [229] R. Li, D. Li, H. Zhang, J. Wang, X. Li, J. Xiao, Growth factors-based therapeutic strategies and their underlying signaling mechanisms for peripheral nerve regeneration, *Acta Pharmacol. Sin.* 41 (2020) 1289–1300.
- [230] L. Zhu, S. Jia, T. Liu, L. Yan, D. Huang, Z. Wang, S. Chen, Z. Zhang, W. Zeng, Y. Zhang, Aligned PCL fiber conduits immobilized with nerve growth factor

- gradients enhance and direct sciatic nerve regeneration, *Adv. Funct. Mater.* 30 (39) (2020) 2002610.
- [231] Y. Ikegami, H. Ijima, Development of heparin-conjugated nanofibers and a novel biological signal by immobilized growth factors for peripheral nerve regeneration, *J. Biosci. Bioeng.* 129 (3) (2020) 354–362.
- [232] H. Zhou, Y. Gong, Y. Liu, A. Huang, X. Zhu, J. Liu, G. Yuan, L. Zhang, J. Wei, J. Liu, Intelligently thermoresponsive flower-like hollow nano-ruthenium system for sustained release of nerve growth factor to inhibit hyperphosphorylation of tau and neuronal damage for the treatment of Alzheimer's disease, *Biomaterials* 237 (2020) 119822.
- [233] S. Ghosh, A. Shrivastava, P. Jha, P. Roy, D. Lahiri, Analysis of neural cell behaviour on anisotropic electrically conductive polymeric biodegradable scaffolds reinforced with carbon nanotubes, *Medical Devices & Sensors* (2020), e10152.
- [234] J. Zhang, X. Zhang, C. Wang, F. Li, Z. Qiao, L. Zeng, Z. Wang, H. Liu, J. Ding, H. Yang, Conductive composite fiber with optimized alignment guides neural regeneration under electrical stimulation, *Advanced Healthcare Materials* 10 (3) (2021) 2000604.
- [235] S. Ghosh, S. Haldar, S. Gupta, A. Bisht, S. Chauhan, V. Kumar, P. Roy, D. Lahiri, Anisotropically conductive biodegradable scaffold with coaxially aligned carbon nanotubes for directional regeneration of peripheral nerves, *ACS Applied Bio Materials* 3 (9) (2020) 5796–5812.
- [236] Y. Chang, M. Chen, S. Liao, H. Wu, C. Kuan, J. Sun, T. Wang, Multichanneled nerve guidance conduit with spatial gradients of neurotrophic factors and oriented nanotopography for repairing the peripheral nervous system, *ACS Appl. Mater. Interfaces* 9 (43) (2017) 37623–37636.